공학박사학위논문

# Maintenance Optimization and Life Cycle Prediction of Systems under Uncertainty

# 불확실성 하에서 시스템의 유지 보수 최적화 및 수명 주기 예측

2019 년 2 월

서울대학교 대학원

화학생물공학부

박 건 희

# Maintenance Optimization and Life Cycle Prediction of Systems under Uncertainty

# 불확실성 하에서 시스템의 유지 보수 최적화 및 수명 주기 예측

지도교수 이 원 보

이 논문을 공학박사 학위논문으로 제출함

2019 년 2 월

서울대학교 대학원

화학생물공학부

박 건 희

박건희의 공학박사 학위논문을 인준함

2019 년 2 월

위 원 장 _____ (인)

부위원장 _____ (인)

위 원 _____ (인)

위 원 _____ (인)

위 원 _____ (인)

## Abstract

# Maintenance Optimization and Life Cycle Prediction of Systems under Uncertainty

Keonhee Park

School of Chemical & Biological Engineering

The Graduate School

Seoul National University

The equipment and energy systems of most chemical plants have undergone repetitive physical and chemical changes and lead to equipment failure through aging process. Replacement and maintenance management at an appropriate point in time is an important issue in terms of safety, reliability and performance. However, it is difficult to find an optimal solution because there is a trade-off between maintenance cost and system performance. In many cases, operation companies follow expert opinions based on long-term industry experience or forced government policy. For cost-effective management, a quantitative state estimation method and management methodology of the target system is needed. Various monitoring technologies have been introduced from the field,

and quantifiable methodologies have been introduced. This can be used to diagnose the current state and to predict the life span. It is useful for decision making of system management.

This thesis propose a methodology for lifetime prediction and management optimization in energy storage system and underground piping environment.

First part is about online state of health estimation algorithm for energy storage system. Lithium-ion batteries are widely used from portable electronics to auxiliary power supplies for vehicle and renewable power generation. In order for the battery to play a key role as an energy storage device, the state estimation, represented by state of charge and state of health, must be well established. Accurate rigorous dynamic models are essential for predicting the state-of health. There are various models from the first principle partial differential model to the equivalent circuit model for electrochemical phenomena of battery charge / discharge. It is important to simulate the battery dynamic behavior to estimate system state. However, there is a limitation on the calculation load, therefore an equivalent circuit model is widely used for state estimation. Author presents a state of health estimation algorithm for energy storage system. The proposed methodology is intended for state of health estimation under various operating conditions including changes in temperature, current and voltage. Using a recursive estimator, this method estimate the current battery state variable related to battery cell life. State of

health estimation algorithm uses estimated capacity as a cell life-time indicator. Adaptive parameters are calibrated by a least sum square error estimation method based on nonlinear programming. The proposed state-of health estimation methodology is validated with cell experimental lithium ion battery pack data under typical operation schedules and demonstration site operating data. The presented results show that the proposed method is appropriate for state of health estimation under various conditions. The suitability of algorithm is demonstrated with on and off line monitoring of new and aged cells using cyclic degradation experiments. The results from diverse experimental data and data of demonstration sites show the appropriateness of the accuracy, robustness.

Second part is structural reliability model for quantification about underground pipeline risk. Since the long term usage and irregular inspection activities about detection of corrosion defect, catastrophic accidents have been increasing in underground pipelines. Underground pipeline network is a complex infrastructure system that has significant impact on the economic, environmental and social aspects of modern societies. Reliability based quantitative risk assessment model is useful for underground pipeline involving uncertainties. Firstly, main pipeline failure threats and failure modes are defined. External corrosion is time-dependent factor and equipment impact is time-independent factor. The limit state function for each failure cause is defined and

the accident probability is calculated by Monte Carlo simulation. Simplified consequence model is used for quantification about expected failure cost. It is applied to an existing underground pipeline for several fluids in Ulsan industrial complex. This study would contribute to introduce quantitative results to prioritize pipeline management with relative risk comparisons

Third part is maintenance optimization about aged underground pipeline system. In order to detect and respond to faults causing major accidents, high resolution devices such as ILI(Inline inspection), Hydrostatic Testing, and External Corrosion Direct Assessment(ECDA) can be used. The proposed method demonstrates the structural adequacy of a pipeline by making an explicit estimate of its reliability and comparing it to a specified reliability target. Structural reliability analysis is obtaining wider acceptance as a basis for evaluating pipeline integrity and these methods are ideally suited to managing metal corrosion damage as identified risk reduction strategies. The essence of this approach is to combine deterministic failure models with maintenance data and the pipeline attributes, experimental corrosion growth rate database, and the uncertainties inherent in this information. The calculated failure probability suggests the basis for informed decisions on which defects to repair, when to repair them and when to re-inspect or replace them. This work could contribute to state estimation and control of the lithium ion battery for the energy storage

system. Also, maintenance optimization model helps pipeline decision-maker determine which integrity action is better option based on total cost and risk.

**Keywords**: State of health ; Lithium ion battery; Reliability ; Monte-carlo simulation ; Limit state function ; failure mode ; underground pipeline

**Student Number**: 2012-23264

# Contents

# List of Figures

# List of Tables

# CHAPTER 1. Introduction

## 1.1. Research motivation

In the generation of great inventions and equipment, the purpose of engineering design is to fulfill its primary function when first manufactured. However, in the generation of contemporary engineering system, that focus is changed. The stability of engineering system over long lifetimes is a significant aspect of large-scale complex systems. These issues are such as flexibility, maintainability, reliability, safety and quality, etc. These properties are not the primary functional requirements of a system's performance, but system impacts with respect to time and stakeholders than are embodied in those primary functional requirements.

Most systems undergo degradation processes due to various causes. Main Causes can include corrosion and erosion of the materials that make up the system, cumulative fatigue, and changes in electrochemical composition. Changes in the state of the system can lead to problems such as decreased productivity and increased risk. However, system uncertainty factors lead to deviation between computational model and real applications. Uncertainty factors are related to accuracy and robustness of engineering problem solution techniques. The source of uncertainty is summarized as follows.[1-3] In real applications, Numerous methodologies have been proposed and utilized to overcome these uncertainties.

**Table 1-1. Uncertainty Sources about system problem**

| Source of Uncertainty | Description |
|---|---|
| Parameter Uncertainty | Factors related to model parameters that are inputs to the mathematical model |
| Parametric Variability | The variability of input variables of the model |
| Structural Uncertainty | Model inadequacy, model bias, model discrepancy, which come from the lack of knowledge of the underlying physics in the problem or several approximations to reality |
| Algorithmic Uncertainty | Numerical uncertainty, numerical errors and approximations per implementation of the computer model. |
| Experimental uncertainty | Observation error, comes from the variability of experimental measurements |
| Interpolation uncertainty | Lack of available data collected from computer model simulations and/or experimental measurements |

This thesis discusses the state estimation technique and systematic interdisciplinary approach for efficient management of two systems.

The first chapter is related to the state estimation of Li-ion batteries, which have been widely used in many fields in recent years. Lithium ion batteries have been highlighted in electric vehicle applications as hybrid energy system and energy storage system for auxiliary device of renewable power generation. The performance, cost and durability of the energy storage are critical for the overall feasibility of a battery system. The most capable cell type is the LiFePO4 / graphite cell, introduced to market recently. It is difficult to estimate the life-time because of highly nonlinear battery ageing mechanisms. State of Health(SOH) has become an important indicator for state of charge and prediction of current life time. The experimental based degradation model demands that a number of cyclic condition such as charging/discharging C-rate, state of charge, temperature, and operating patterns. However, the prognostic method about life time of Li-ion batteries for various application has still uncertain. Uncertainty management for battery diagnostics and prognostics is another important factor that needs to be considered [4] because the difference between experimental validation and real application system. The cell to cell variation in manufacturing step and parameter uncertainty in a specific battery model are representative source of uncertainties. The estimation of battery state variables can be accurate for specific cell under calibration

condition but not so can predict well for other cell in same operating condition. Therefore, uncertainty factors in battery state estimation algorithm should be considered appropriately. However, the empirical models are expensive to construct, and have limitations in that they can be guaranteed only for specific battery compositions and manufacturers. Hence, reliable estimation of battery life as online adaptive model maintain the battery cell performance during operating hours.

The second part is about to set the reliability based pipeline maintenance model. Pipelines are the most economical and safe way to transport energy or transport materials. There are various piping safety evaluation methods to evaluate reliability before pipe failures occur in pipeline. The specifications of the gas pipeline used in Korea and the specifications of the materials and environment are different. In addition, the buried pipelines in the major national industrial complexes in Korea account for 65% (687 km) of long-term piping for more than 15 years. Due to the nature of domestic industrial complexes, there is a high possibility that the fire and explosion will cause great casualties and damage to property. Therefore, a systematic management method is needed. In general, facility management refers to predicting the possible damages of facilities designed and manufactured with a design life, and predicting and managing the lifespan in an appropriate manner. The main threats to the safety of piping include external interference from other constructions, external corrosion of pipes,

construction defects, ground movements, and operational errors. Accidents of high-pressure gas pipelines buried domestically and abroad are caused by aged piping, which often causes human injury or environmental pollution. Overseas, high-pressure gas pipeline management is under the management of European Gas Pipeline Incident Data Group(EGIG) and Pipeline and Hazardous Materials Safety Administration.(PHMSA). The Integrity Management Program(IMP) has implemented the US 49 CFR 195.452 guideline on the High Consequence Area to manage its reliability [5]. This procedure has the effect of preventing the danger that may occur in the piping in advance. On the other hand, the Korea industrial complex has short and dense underground pipeline environment. Therefore, there is a problem of applicability to proceed with advanced reliability management procedures. In addition, industrial complexes should consider various products. On the other hand, most of the buried pipe management standards are uncertain due to the lack of data and the subjective judgment of experts. In addition, even if a certain risk reduction activity is not quantified, the effectiveness is difficult to judge. All mitigation activities from inspection, excavation, repair, and patrols will lead to an increase in management costs, so screening process for high-risk piping is necessary. Therefore, pipeline management decision maker should concern the current quantitative risk about pipeline and the effect of risk mitigation activities. Structural Reliability Analysis(SRA) provides a way to determine the benefit between

the value of reduced risk and the costs of the activities associated with that mitigation using cost model. This framework can help evaluate the probability of failure accurately as well as the consequences related with pipeline failure.

## 1.2. Research objectives

The objective of this thesis is to propose an estimation method of life-cycle variable for Li-ion battery and aged underground pipeline. First topic is battery state of health estimation(SOH) algorithm for Li-ion battery. This method is validated based on each cell as well as pack data for various operation data. In the previous studies, only the EV data was evaluated, but this prediction algorithm in a more diverse operating environment was evaluated. Thesis propose an efficient algorithm for Energy storage system for multi-cell system. A number of uncertainties must be considered for risk assessment management of aging underground piping. There are some uncertainty factors such as measurement error of inspection and pipeline failure model error. Limit state functions are defined based on a probability model of the Gauge-dent and corrosion defects using stress calculation model. For this, maintenance optimization can be carried out based on reliability, consequence and cost modeling, using simulation technique. Based on the piping data of Ulsan Industrial Complex, the case study was conducted to demonstrate the usefulness of the methodology.

## 1.3. Outline of the thesis

Chapter 1 provides the research motivation and the objective of the thesis. And Chapter 2 describe the design of online SOH Estimation algorithm derived mixing and modified previous method. The accuracy of the proposed methodology was verified from cell and pack data for ESS operation. Chapter 3 explains the underground pipeline failure modeling with uncertainty. And several case studies show examples of prioritizing pipeline based on risk. In Chapter 4, maintenance mitigation model and reliability target model is formulated for maintenance optimization. It describes that this framework help company find the cost-effective mitigation action in various pipeline conditions. Chapter 5 summarizes the conclusion and the suggestion for the future works.

# CHAPTER 2. Lithium ion battery modeling and state of health Estimation

## 2.1. Background

Lithium-ion batteries have been widely applied in a variety of renewable energy storage fields, providing high capacity, high energy density, and higher open circuit volt-age (OCV) [6, 7]. In managing safety, reliability, and efficiency of Li-ion battery systems, the battery status is necessary to be monitored and maintained in an accurate way. In order to ensure these features, a battery management system (BMS) is a promising solution, and the accurate estimations of battery capacity, state of charge (SOC), and state of health (SOH), essentially governed by the BMS are core characteristics when operating Li-ion battery systems [8-10]. Energy storage system (ESS) using Li-ion batteries involves a BMS as an essential component not only to manage data acquisition/storage, capacity measurement, and SOC estimation, but also to monitor the battery system for safe operations with on-line control, including the protection from sudden events [11]. Among these functions of BMS, the SOC estimation is one of the important dependency with battery current life. In addition, controlled measures of real-time SOC estimations enable BMS to prevent the batteries from hazardous events such as over-charged/discharged and over-heating events [12]. The accuracy of SOC estimation is affected by battery degradation. In this sense, sole SOC estimation may cause errors that

may have a direct influence on SOH calibrations [13].Therefore, coestimation of SOC and SOH should be considered as accurate estimation of Li-ion battery aging.

## 2.2. Literature Review

Coulomb counting has been extensively used to evaluate SOC values and calculate remaining capacity which is obtained from accumulated charges during charging or discharging operations. This method is not difficult for calculations, but it needs an accurate value of initial SOC. In the meantime, OCV-based method is only accurate for rest-time periods on low current operations, and not effective for moderate or high current operations [12] Adaptive SOC estimation approaches that are neural network [14], fuzzy logic [15-17] EKF [18, 19], etc. have been employed to address the accuracy issue of SOC estimation, based on the coulomb counting and open circuit voltage based method [20-23]. In addition, the regression model is used to predict the state of health and Remaining useful life(RUL) based on data-driven approach. There is also a model for predicting future capacity fade by constructing a charge decay model using a nonlinear mixed effect model.[24] Recently, Datong Liu applied applied the Expectation and Maximization(EM) algorithm to estimate the parameters to construct the battery capacity fade regression model. This is possible with long term prediction of SOH based on the Gaussian Particle Filtering Regression Model[25, 26]

### 2.2.1. Battery model

Electrochemical cell dynamic voltage models such as first principle model and equivalent circuit model(ECM) are used for Li-ion batteries in terms of current, voltage, and temperature variables [27]. The models such as first principle model and mathematical model based on electrochemistry, thermodynamics, and transport phenomena are accurate models that are composed of several partial differential equations and ordinary differential equations. [28] However, the computational loads are heavy and the computations take longer time than each of the SOC estimation intervals does.

Battery circuit model used in this work is appropriate to be implemented in BMS algorithm, since the model expressed by a simplified circuit with a single resistance and a single RC and 2RC components remarkably lightens the computational loads and ensures its accuracy in managing current and voltage that are the required variables [29]. In regard to the simplified circuit, Hu et al. 2012 conducted a comparative study about battery dynamic performance of twelve equivalent circuit models and reached the conclusion that the first-order RC model is preferably chosen for Lithium-nickel-manganese-cobalt oxide (LiNMC) type cells, regarding model complexity, accuracy, and robustness [30]. However, 2-RC model is also used in this study for accuracy comparison. The circuit model represents electrochemical features of the battery cells by means

of current and voltage as monitored variables at different temperature conditions. In Table 1, components and their meanings of the first-order equivalent circuit model and Second order equivalent circuit model are described. The model consisting of each RC-circuit that implies an electric double layer and diffusion is displayed in Figure 1.

R0 means internal resistance as a single resistance in electrode, and R and C are expressed as interfacial resistances and capacitor, induced by electric double layer phenomena that take place at an interfacial layer between electrode and electrolyte in a battery cell. Related to R and C variables, α representing and β standing for $e^{-\frac{\Delta t}{RC}}$ are used as substituted terms. Also, V0 is OCV, dependently correlated to the nominal SOC. These estimated parameters are characterized in the equivalent circuit model, and static / dynamic properties in a battery cell are featured. As following Kirchhoff's circuit law, overall currents in the circuit model can be defined as Eq. 1.

$$\mathrm{I} + I_2 + I_3 = 0 \quad (1)$$

With the use of a single resistance and a single RC circuit, the circuit model can be derived as Eq 2.

$$\frac{d}{dt}(\mathrm{V} - V_0) + \frac{(V - V_0)}{RC} = \frac{I}{C}\left(1 + \frac{R_0}{R}\right) + R_0\frac{dI}{dt} \quad (2)$$

and by using an integrating factor and an integral in terms of time, Eq. 3 can be obtained.

$$\mathrm{V} = \frac{Q(0)}{C} e^{-t/RC} + V_0 + IR_0 + \frac{1}{C}\int_{\xi=0}^{\xi=t} (I(\xi) e^{-\frac{t-\xi}{RC}}) d\xi \quad (3)$$

In a few moments when SOC algorithm starts running, it is supposed that there is no polarization behavior, and thus, Q(0) should be considered as zero. Next, V0 and current input data with regular time intervals are taken to formulate a discrete formula which is considered as a recursive form. The circuit model equation developed by Verbrugge [31] is expressed as Eq. 4

$$V_k = V_{o,k} + I_k R_0 + \alpha I_k \Delta t + \beta\left(V_{k-1} - V_{0,k-1} - I_{k-1} R_0\right) \quad (4)$$

This voltage model was used as implemented in our previous work. That only consider a dynamic battery modeling for an EV application field, however. In this model, I is current known as an input variable, and V is voltage known as an output variable. Also, Δt is a time interval for input data entered into the circuit model, and the time interval measured in an experiment was assumed as a constant value during the voltage estimation period. Eq. 4 is a final terminal voltage equation, and it is possible to calculate a terminal voltage through the circuit model recursively that produces an estimated voltage of a previous step and an ongoing voltage variable as a function of time.

Because the observer technique is used in the modeling process described below, the state-space form for each ECM is summarized as follows. [32]

(1st ECM)

$$\begin{bmatrix} \dot{SOC} \\ \dot{V_p} \end{bmatrix} = \begin{bmatrix} 1 & 0 \\ 0 & 1 - \frac{1}{R_p C_p} \end{bmatrix} \begin{bmatrix} SOC \\ V_p \end{bmatrix} + \begin{bmatrix} -\frac{1}{C_{cap}} \\ \frac{1}{C_p} \end{bmatrix} i \quad (5)$$

$$V = h(OCV, V_p) - R_0 i = OCV - V_p - [R_i] i \quad (6)$$

$$A = \begin{bmatrix} 1 & 0 \\ 0 & 1 - \frac{1}{R_p C_p} \end{bmatrix}, \mathrm{B} = \begin{bmatrix} -\frac{1}{C_{n,k}} \\ \frac{1}{C_p} \end{bmatrix}, \; C = \begin{bmatrix} \frac{\partial h_k(SOC)}{\partial x_k} & 0 \\ 0 & -1 \end{bmatrix}, \mathrm{D} = [R_i] \quad (7)$$

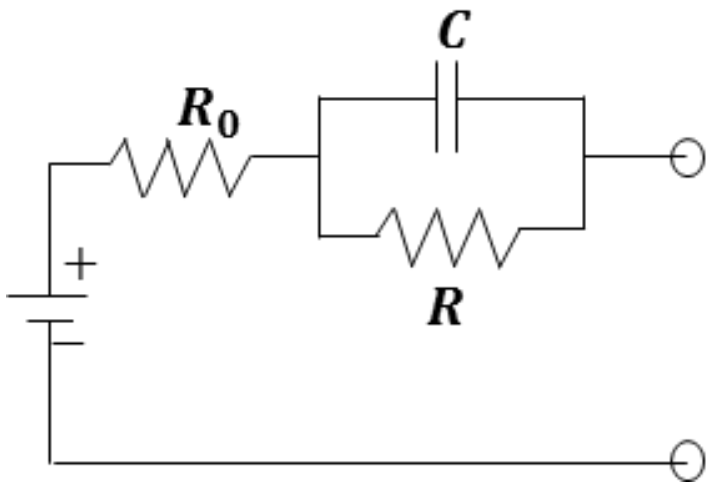


**Figure 2-1. First order RC Equivalent Circuit Model**

**Table 2-1 Description of Equivalent Circuit Model**

| Parameter | Description |
|---|---|
| $V_0$ | Initial open circuit voltage |
| $R_0$ | Ohmic resistance / lumped series resistances for the solid and liquid phases |
| R | Lumped interfacial resistances |
| C | Interfacial capacitances |
| $\alpha$ | 1/C |
| $\beta$ | exp-($\Delta t/RC$) |

### 2.2.2. Qualitative comparative review of state of health estimation algorithm

SOH(State of health) can be defined two ways. [33] First, battery impedance may be used to indicate battery SOH. This is based on power fade.

$$SOH = \frac{R_i}{R_0} \times 100\% \quad (8)$$

Where $R_i$ is the certain time impedance measurement that is varied with the repeated cycles, and $R_0$ is the initial impedance. In ECM, impedance has similar characteristic with ohmic resistance. Therefore, R parameters can be introduced to determine for online SOH estimation algorithm

Second way is based on battery capacity C.

$$SOH = \frac{C_i}{C_0} \times 100\% \quad (9)$$

Where $C_i$ is the ith capacitance value degradated with cycles and $C_0$ is the initial capacity in fresh cell.

In SOH predictions, durability opened-loop methods and battery closed-loop methods are generally used as model-based SOH estimation methods [34] While the durability opened-loop methods estimate the increases of internal resistance and terminal voltage status, the battery closed-loop methods are used to identify battery capacity and internal resistance with least square methods, Kalman filtering, and other adaptive algorithms. Most of the SOC/SOH

estimation methods have been developed in a separate way rather than a combination method. As mentioned above, only usage of SOC estimation method is likely to cause non-negligible errors and to mislead battery SOH calibrations, and hence, it results in the inaccurate estimations of the battery current states [35]. In this sense, the on-line and simultaneous estimation of both SOC and SOH can apparently be practical to reach accurate estimations in various circumstances. Thus, the battery states, even regarding the battery degradations can more accurately be monitored in real-time to predict the life-span and to determine the replacement time.

The advantages and disadvantages of each methodology reported in the literature are summarized as follows

**Table 2-2 Summary of qualitative comparison about state of health estimation methods**

| | **Simplified Parameter Estimation Based** | **Kalman filtering based approach** | **Sliding mode observer** |
|---|---|---|---|
| Pros | Simple<br>Fast Computation | Closed Loop<br>accuracy | Closed Loop<br>Relatively low<br>dependency of battery model<br>Robust behavior |
| Cons | Open loop method<br>High Initial SOC dependency<br>Error Accumulation | Highly dependent on model<br>accuracy<br>complex matrix calculation | Computational Expensive |

Since the types and specifications of batteries used in previous studies are different, it is impossible to make reasonable comparison of accuracy. SoH prediction methodology has been developed with accuracy of around 3-10%. Various methods have been proposed, but no quantitative comparison has been made under the same model conditions as the same input data. It is necessary to analyze how the predictive characteristics of each methodology affect quantitatively.

## 2.3. Previous estimation algorithm

SOH values define as the Capacity fading or power fading. The replacement-time estimation about battery in ESS or HEV is an important issue for the manufacturer and system operator. However, direct measurement of the performance with a BMS sensor was a difficult problem. And offline method is costly and has the disadvantage that regular monitoring is difficult if the system is isolated such as energy storage system in conjunction with photovoltaic system. In this chapter, previous State of health estimation method are suggested for on-line estimation of actual battery performance.

### 2.3.1. Nonlinear State estimation method

System is must be observable to ensure that the state estimate converges to the true value. Therefore, observability and stability of system is needed for

applicability of various state estimation algorithm. Observability matrix of the linear time invariant system(LTI) can be formed [36]

$$O_1 = \begin{bmatrix} C \\ CA \\ CA^2 \end{bmatrix} \quad (10)$$

If such a matrix is always full rank under any operating condition, the battery model is observable and it is possible to estimate the internal state. The output equation is nonlinear because of SOC-OCV relation of Li battery. However, Voltage and SOC can be approximated as linear over operating ranges of SOC and current that are typically seen in a ESS and HEV application(20-90% SOC and $\pm$10C). The OCV curves for NCM+LMO/GC and NCM+NCA/LFP are roughly linear over certain SOC ranges. Applying piece-wise linear assumption in this region, the output equation becomes linear. The number of states and the number of states in the Observability matrix are the same. When 1 RC ladder equivalent circuit model is applied, observability and stability test is as follows.[32]

$$\dot{\hat{x}} = A\hat{x} + Bu + kp_i(\mathrm{y} - \hat{y}) + \omega \quad (11)$$

$$\dot{\omega} = ki_i(y - \hat{y}) \quad (12)$$

Where $\omega$ is the integral of the difference between the measured output y and the output provided by the observer $\hat{y}$. The observer error is defined by

$$\tilde{e} = \hat{x} - x \quad (13)$$

So that

$$\begin{pmatrix} \dot{\tilde{e}} \\ \dot{\omega} \end{pmatrix} = A_e \begin{pmatrix} \tilde{e} \\ \omega \end{pmatrix} \quad (14)$$

$$A_e = \begin{bmatrix} A - kp_i C & 1 \\ -ki_i C & 0 \end{bmatrix} \quad (15)$$

Hurwitz matrix $A_e$ means that the observer system would asymptotically converge. Therefore, this system can be applied observer technique to estimate internal state variable.

The Kalman filter is a well known tool for state estimation of dynamic systems, being the optimal state observer for linear systems with quantifiable process and signal noise that is uncorrelated, white, and Gaussian. [18, 37]. Since the output voltage equation are nonlinear, an EKF is used, which calculates the feedback gain by approximating the nonlinear system as a linear time varying system. During the prediction step, the model is simulated open loop to obtain a state prediction and output prediction. During the correction step, a correction is applied to the state prediction using proportional feedback from the measured output. The proportional gain is a function of the process and sensor noise covariance. In large uncertainty system, state estimate should depend more on the measurement feedback. Contrary, if there is large uncertainty in the measurement, the gain will tend to be low.

### 2.3.2. Sliding mode observer

Conventional SMOs with the constant switching gains for the SOC estimation have demonstrated the robustness to compensate modelling errors and uncertainties with the properly selected switching gains.[38, 39]

Incorrect Switching gains are a major cause of the chattering phenomena of the SOC. Therefore, an adaptive gain sliding mode observer(AGSMO) is needed for accurate state estimates.

$$\dot{\hat{V}}_t = -a_1\hat{V}_t + a_1 h(SOC) - b_1 I + \hat{\Gamma}_1 sgn(e_{vt}) \quad (16)$$

$$\dot{\widehat{SOC}} = -a_2\hat{V}_t - a_2 h(SOC) + a_2\dot{\hat{V}}_p + \hat{\Gamma}_2 sgn(e_{OCV}) \quad (17)$$

$$\dot{\hat{V}}_p = -a_1\hat{V}_p + b_2 I + \hat{\Gamma}_3 sgn(e_{vp}) \quad (18)$$

$\hat{\Gamma}_1$, $\hat{\Gamma}_2$, $\hat{\Gamma}_3$ are adaptive switching gain, $\hat{\Gamma}_1 = \gamma_1|e_{vt}|, \hat{\Gamma}_2 = \gamma_2|e_{ocv}|, \hat{\Gamma}_3 = \gamma_3|e_{vp}|$ where the terms $\gamma_1, \gamma_2, \gamma_3$ are positive constants that should be choosen suitably small so that they can ensure the adaptation speed of the switching gains for state errors convergence while preventing the corresponding $\hat{\Gamma}_i$ from becoming too large and guaranteeing suitable bounded magnitude of the switching gains. And sgn is the signum function

$$\text{sgn}(e_{vt}) = \begin{cases} +1, & e_{vt} > 0 \\ -1, & e_{vt} < 0 \end{cases} \quad (19)$$

$$\dot{\hat{e}}_{Vt} = -a_1 e_{Vt} + a_1 e_{ocv} + \Delta f_1 - \hat{\Gamma}_1 sgn(e_{vt}) \quad (20)$$

$$\dot{\hat{e}}_{soc} = a_2 e_{vt} - a_2 \kappa e_z + a_2 \mathrm{e}_{vp} + \Delta f_2 - \hat{\Gamma}_2 sgn(e_{SOC}) \quad (21)$$

$$\dot{\hat{e}}_{vp} = -a_1 e_{vp} + \Delta f_3 - \hat{\Gamma}_3 sgn\left(e_{vp}\right) \quad (22)$$

And Lyapunov function is formulated as follows.

$$V_1 = \frac{1}{2}\left(e_{vt}^2 + \gamma_1^{-1}\tilde{\Gamma}_1^2\right) \quad (23)$$

$$\dot{V}_1 = |e_{vt}|(a_1|e_{ocv}| + |\Delta f_1| - \Gamma_1) \quad (24)$$

Therefore, there exists an unknown finite non negative switching gain $\Gamma_1$ such that $\Gamma_1 > a_1|e_{ocv}| + |\Delta f_1|$, leading to $\dot{V}_1 < 0$ which satisfies the second method of Lyapunov stability theory. The terminal voltage error as the sliding variable asymptotically converges to zero as time tends to infinity. In other words, the sliding surface is reached during the sliding motion as the sliding variable is equal to zero, where the sliding surface is defined as $e_{vt} = 0$. After each equation is substituted into sliding surface condition, a set of the AGSMO equations are obtained.

$$\dot{\hat{V}}_t = -a_1 \hat{V}_t + a_1 h(SOC) - b_1 I + \hat{\Gamma}_1 sgn(e_{vt}) \quad (25)$$

$$\dot{\widehat{SOC}} = -a_2 \hat{V}_t - a_2 h(SOC) + a_2 \dot{\hat{V}}_p + \hat{\Gamma}_2 sgn\left(\left\{\left(\frac{\hat{\Gamma}_1}{\kappa a_1}\right) sgn(e_{vt})\right\}_{eq}\right) \quad (26)$$

$$\dot{\hat{V}}_p = -a_1 \hat{V}_p + b_2 I + \hat{\Gamma}_3 sgn\left(\left\{\left(\frac{\hat{\Gamma}_2}{a_2}\right) sgn(\left\{\left(\frac{\hat{\Gamma}_1}{\kappa a_1}\right) sgn(e_{vt})\right\}_{eq})\right\}_{eq}\right) \quad (27)$$

### 2.3.3. Proposed Algorithm

Generally, Energy storage system is based on pack and cell unit, and can monitor cell balancing, voltage and current data by mounting BMS. In most literature studies, the SOH algorithm is verified based on cell unit pulse pattern and degradation data. However, the proposed algorithm is validated with the actual application site data and cell operation data simultaneously. The data obtained from the sensor is pre-processed by the data of the unit cell / pack, and the measurement error occurring here is defined as the system factor, $\eta$, to consider the characteristic of the system. The system factor is minimized by minimizing the error between stored SOC and Coulomb counting. The SOH algorithm is designed to be easily applied from the outside to the BMS built in the real application site. The SOC is estimated using the EKF and the SOH is designed to improve the accuracy by estimating the capacity fade using recursive least square parameter optimization. The objective function of recursive least square method is errors between the battery model voltage and the measured voltage. The ECM parameters are fully dependent on operating conditions, such as SOC, current, and temperature, but the extractions of the model parameters are not necessarily involved in parameterizing all the operating conditions. For example, the battery system in ESS is not considered to fully charge or discharge in the range of 0 ~ 100% of SOC, since the ESS operations are run on the range of 20 ~ 80% of SOC in many cases.

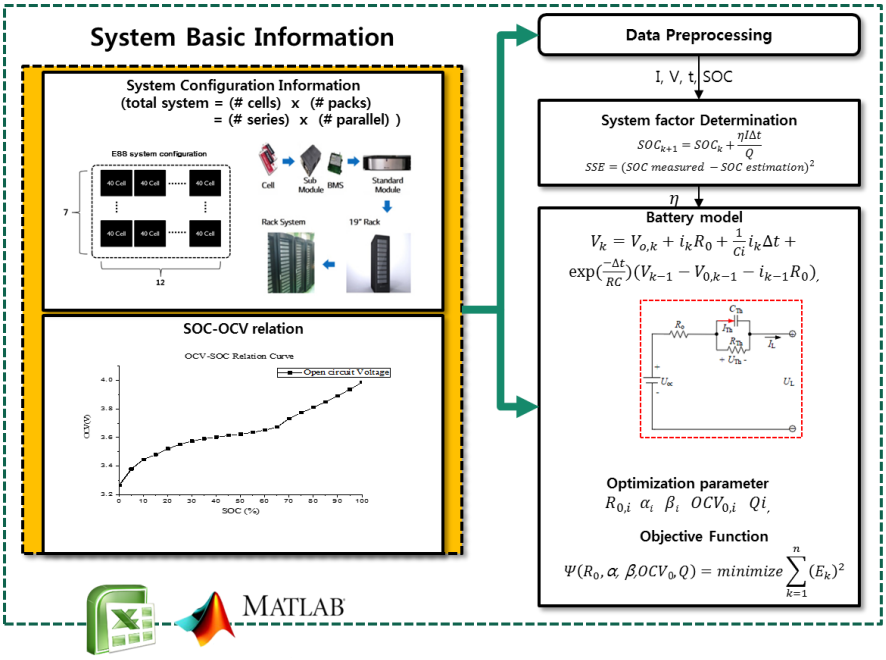


**Figure 2-2 Concept of proposed SOH estimation methods for Energy storage system**

In the SOH estimations mainly considering the SOC 20 ~ 80% range, the data acquisition of voltage ($V_k$ ), current ($I_k$), and time ($t_k$)is completed by BMS in a continuous way to collect n data set. For the data collection, n=100,000 data set were gathered to validate the SOH algorithm and to reflect the daily degradation properties of the battery system.

$$SOH_i(\%) = \frac{Q_{max}(aged\ capacity)}{Q_{max}(Fresh\ Cell\ capacity)} \times 100 \quad (28)$$

When the initially optimized parameters are extracted to provide the SOH values as using the ratio of $Q_{max}$(aged) to $Q_{max}$(Fresh cell) shown in Eq. 28, initial parameter constraints of $R_0$, α, β, $OCV_0$, and Q are determined in the SOH estimation algorithm for the next parameter optimizations. The constraints of internal battery state variables are shown in Eq.29-33. And, the boundary values of R0, α, and β parameters are defined in the extent of the parameter estimated values that are dependent on current, temperature, and SOC conditions. In the case of $OCV_0$, the constraint is established by setting the voltage deviation (± 0.5 V), counting from an initial terminal voltage. The constraints for Q is determined by using the 10% lower limit than SOH 80% and the 20% upper limit than SOH 100% whose limitations are applied to the batteries used in this work.

$$R_{0,LL} \leq R_0 \leq R_{0,UL} \quad (29)$$

$$a_{LL} \leq a \leq a_{UL} \quad (30)$$

$$\beta_{LL} \leq \beta \leq \beta_{UL} \quad (31)$$

$$V_{0,k} - \delta \leq V_{0,k} \leq V_{0.k} + \delta \quad (32)$$

$$Q_{LL} \leq Q \leq Q_{UL} \quad (33)$$

$$\Psi(R_0, \alpha, \beta, OCV_0, Q) = minimize \sum_{k=1}^{n} (V_{e,k} - V_{m,k})^2 \quad (34)$$

As minimizing sum of square error(SSE) given in Eq. 34, the objective function is used to optimize the parameters that are satisfied with the constraints defined above. In the SSE equation, $V_{e,k}$ means the kth estimated voltage which is an experimental battery voltage, and $V_{m,k}$ represents the kth modeling battery voltage. The parameter estimations involve the nonlinear mathematical functions in using a nonlinear programming method. The method used here is an interior trust region approach for nonlinear programming in a MATLAB simulation environment with a lsqnonlin function. While the interior-reflective Newton method is necessary to solve quadratic programming sub-problem, the advantage of interior-trust region method is that it does not require solving the sub-problem, and simply updates the trust region size, in addition to maintaining the feature of the interior-reflective Newton method, which is able to find a solution without active set. Thus, using the interior trust region method, computational load is remarkably reduced, and the accuracy of a solution is guaranteed.

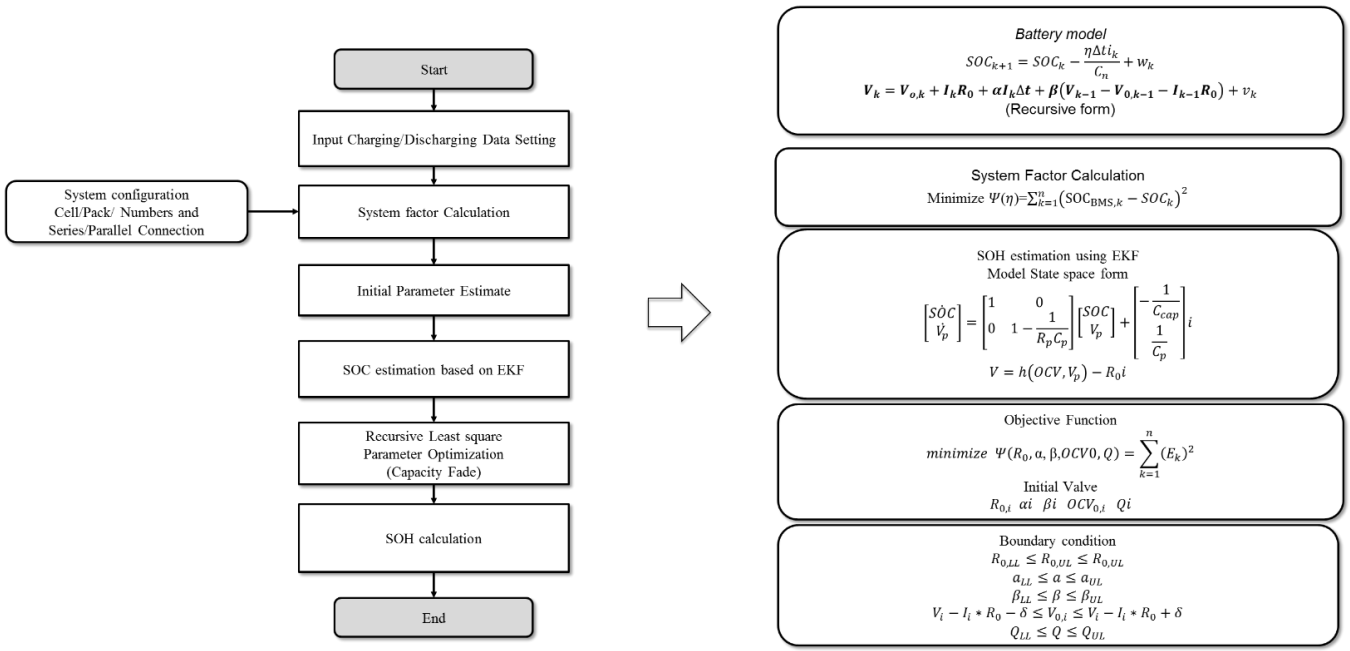


**Figure 2-3 Proposed SOH Estimation algorithm for various sites**

The SOH estimations are accomplished by the steps, shown in Figure 2-2. As a part of the SOH estimation, the k+1th $SOC_I$ calculations can be obtained from the manner that currently measured value, $SOC_{v,k}$, is added to the kth integrated current with time intervals divided by total battery capacity, given by Eq. 8.

In the SOH estimations, there are five optimization variables. $R_0$ and $\alpha$, $\beta$ are general battery parameters. Q is a parameter for a SOH indication. $OCV_0$ is a parameter to guess a $SOC_0$. The appropriate use of a $SOC_0$ determines the accuracy of a SOH estimation. Based on 1st cycled voltage pattern taken from the tested battery, an optimized $OCV_0$ parameter provides an initial SOC value for the next parameter optimization in an efficient way where the parameter optimization does not necessarily take rest times to avoid the polarization effects, which are time-consuming. Therefore, the $OCV_0$ parameter optimization is likely able to ensure the accuracy of an initial SOC estimation even in a long-cycled battery.

### 2.3.4. Uncertainty Factors for SOH estimation in ESS

There are several types of uncertainty factors for reliable battery state estimation. These can be classified as (a) measurement uncertainty, (b) algorithm uncertainty, and (c) environmental uncertainty, (d) model parameter uncertainty, and (e) model uncertainty. Measurement uncertainty is related to current and voltage measurement error. Sensor noise term is typically

considered in KF technique. Algorithm uncertainty focuses on accuracy of numerical algorithms for estimating the battery hidden states. This technique is gradually improve and involves such as EKF, sigma point KF, Unscented KF, Particle Filter etc. Environmental uncertainty is the temperature and abrupt operating variations. Model parameter uncertainty is mainly cause by the manufacturing tolerance resulting in the cell to cell variability. However, there is a lack of systematic approach to characterize the model parameter uncertainty. Model uncertainty is caused by the deviation caused by the assumption that there is no error.

In this study, we focus on estimation of SOH through capacity fade estimation among battery performance forecasts. Since the target system is an energy storage system, it is a large energy storage system consisting of many cell and pack combinations. Since the data input source is often a large scale rather than a cell, uncertainty occurs rather than simple measurement noise.The difference between model terminal voltage and real terminal voltage becomes model uncertainty. Considering the computational load, the ECM selected when online state estimation is needed is a low fidelity model, so consideration of model uncertainty should be more essential. In addition, parameter uncertainty is the realization of the physical uncertainty in the specific ECM. The model parameters include the cell-to-cell variability mentioned earlier in

the ESS system and should be appropriately quantified. In order to consider this, the existing model is calibrated considering the model uncertainty.

$$SOC_{k+1} = SOC_k - \frac{\eta \Delta t i_k}{C_n} + w_k \quad (35)$$

$$V_k = OCV(SOC_k) - i_k R + h_k + \delta\left(i_k, SOC_k, C_{n,k}\right) + v_k \quad (36)$$

Where $h_k$ is the polarization voltage drop, $\delta$ is the model uncertainty. KF Techniques takes into account the estimation of the measurement noise, assuming that Gaussian noise is included in the model. The PF has a good predictability of the state probability density function, but it has a disadvantage of large computational load. Therefore, applying EKF can more accurately predict state variables such as SOC compared to the Coulomb counting method.

## 2.4. Data acquisition

The training and validation data set of Li-ion battery is from industry-academia collaboration program. ESS cell Data is performed by KTC(Korea Testing Certificate). The operation data of the demonstration sites were obtained from the micro grid auxiliary power system and ESS sites for peak shaving, respectively.

### 2.4.1. Lithium ion battery specification

In this paper, we consider all aspects of the SOH prediction algorithm in terms of applicability, accuracy, and simplicity. Therefore, the Li-ion Battery Specification for data used for cell verification and demonstration site verification is different. The specifications of the batteries used in this case are as follows.

**Table 2-3 The Cell Specification of Validation**

| Type | Test A | Test B | Test C |
|---|---|---|---|
| Data Type | Bat 1 | Bat 2 | Bat 3 |
| Chemistry | NCM+LMO/GP+GC | NCM+NCA/LFP | LMO / GC |
| Nominal Capacity(Ah) | 21 | 88 | 75 |
| Charging Voltage | 4.2 | 48 | 67.2 |
| Nominal Voltage | 3.75 | 43.2 | 59.2 |
| Standard Charge/Discharge rate | 0.5C | 1C | 2C |
| Max Charging/Max Discharging | 3.0C(63A)/5.0C(105A) | 3.0C(63A)/5.0C(105A) | 2.0C(150A)/2.0C(150A) |
| Operating temperature | 0-45(Charging)<br>-20-60(Discharging) | -10~+60 | -10~+55 |
| Application | EV/ESS | PV Auxillary Power | Peak Shaving |

### 2.4.2. ESS Experimental setup

The development of an efficient SOH model using an equivalent circuit involves input parameters such as current, internal resistance, and OCV0, and there is one output parameter which is voltage. Experimental measurement of the battery properties is crucial to approaching a realistic estimation of SOH model parameters, and hence, an SOH estimation model can provide more reliable output values. There are two specific goals in applying experimental results to the implementation of the SOH estimation model. One goal is to extract reliably estimated parameters necessary for establishing the SOH model, and the other is to obtain charge and discharge profiles of a battery being degraded through degradation experiments.

In this study, pouch-type cells of lithium-ion battery (LiNMC+LMO type battery), having 253 mm in width and 172 mm in length, manufactured by Enertech International Co., Ltd were used for all experiments with nominal capacity of 21.0 Ah and nominal voltage of 3.75 V. Constant current experiments were carried out to examine the linearity of SOC-OCV patterns and to discover any correlations between SOC and OCV in various operating conditions. 0.1 C-rate for charging or discharging current of the tested batteries is employed to change each 10% of SOC either upward or downward in the

SOC range of 0 ~ 100%, and an enough rest period (> 15 min) is considered to avoid the polarization effects and to have the stabilized OCV values.

Pulse pattern experiments were introduced to characterize the polarization behaviors of the tested batteries shown in Figure 3 and to verify the robustness of the SOH model with high pulse current in various operating conditions. During a cycle of the pulse pattern, a rated pulse current for 10 seconds is adopted, and a rest period for 60 seconds is used to ensure the removal of the polarization effects derived from an electric double layer inside the battery. The ambient temperatures are used as 273 K, 298 K, and 323 K. Also, ten intervals in the SOC% range for pulse current patterns are considered to achieve reasonable DC−IR test results.

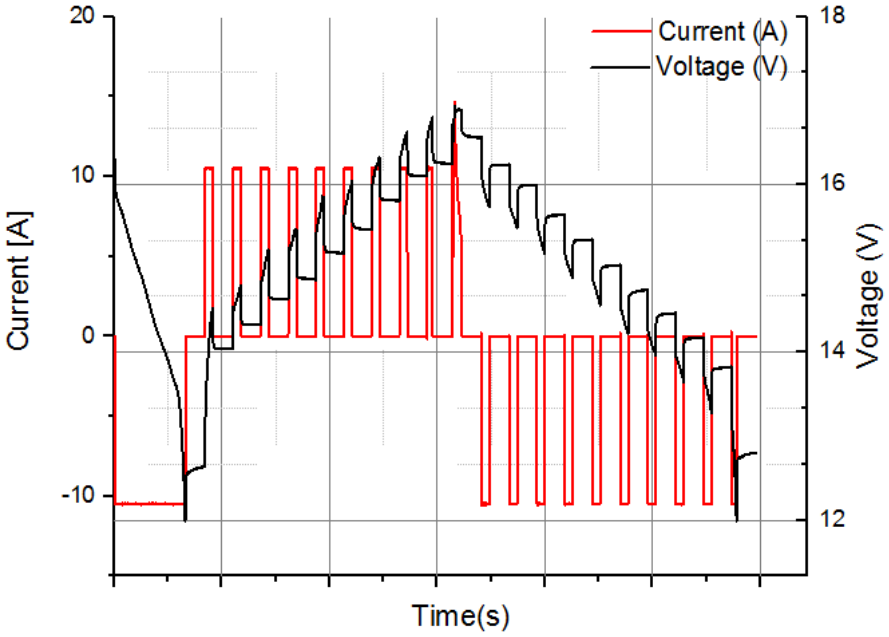


**Figure 2-4 Polarization behaviours about experimental pulse pattern**

Battery degradation tests are needed to observe battery life patterns that are dependent on the battery degradation states, reflecting internal resistance and capacity variations of the battery. Degradation experiments were conducted by running out of the battery life in which various rated conditions (e.g. max 5 C) for charging or discharging operations were used to degrade the battery at 273 K, 298 K, and 323 K. The tested battery life engaging with the harsh operating conditions results in the battery end life (～80% of SOH), corresponding to ≤ 1000 cycles. This degradation condition presumably corresponds to an experiment condition where the tested battery becomes degraded by ～2500 cycles, leading to SOH ～80%. Thus, the designed pulse currents are regularly flowed in and out of the tested battery as charging or discharging for the degradations. During the current pulse pattern tests, constant current (CC) experiments were also included to monitor whether any particular voltage patterns and any changes of the SOC-OCV correlations take place. The CC tests were randomly chosen, for example, when increasing current pulse cycles up to 300th cycle for total 4 times, and the tests are carried out at every 100th cycle that starts from 300th cycle up to ～1000th cycle.

The SOH model verifications have been conducted to establish model reliability and robustness by optimizing the operation voltage patterns of a representative energy storage system for the purpose of peak shaving energy balance, targeting an efficient energy management. In designing the verification

tests, electric power load patterns are presumably interpreted by using electric rates, provided by Korea Electric Power Corporation (KEPCO). Based on the interpretations, possible operation patterns of the battery system in ESS have been evaluated and determined. Moreover, as referring to the report released by Korea Energy Economics Institute (KEEI) on electric load patterns, it is noted that the electric loads at 11 AM and 3 PM dis- play higher peak loads in a daily operation. Table 2-4 summarizes ESS operation conditions in which the SOH model contributes to optimizing an efficient energy management.

**Table 2-4 Summary of ESS operation conditions based on electric rates charge. (Test A)**

| Classification | Time | Operation | Status |
|---|---|---|---|
| Off-peak | 23:00 ~ 09:00 | 4.2A (0.2C) | Charge |
| Mid-peak | 09:00 ~ 10:00 | Rest | - |
| | 12:00 ~ 13:00 | 21A (1C) | Charge |
| | 17:00 ~ 23:00 | Rest | - |
| On-peak | 10:00 ~ 12:00 | 8.4A (0.4C) | Discharge |
| | 13:00 ~ 17:00 | 4.2A (0.2C) | Discharge |

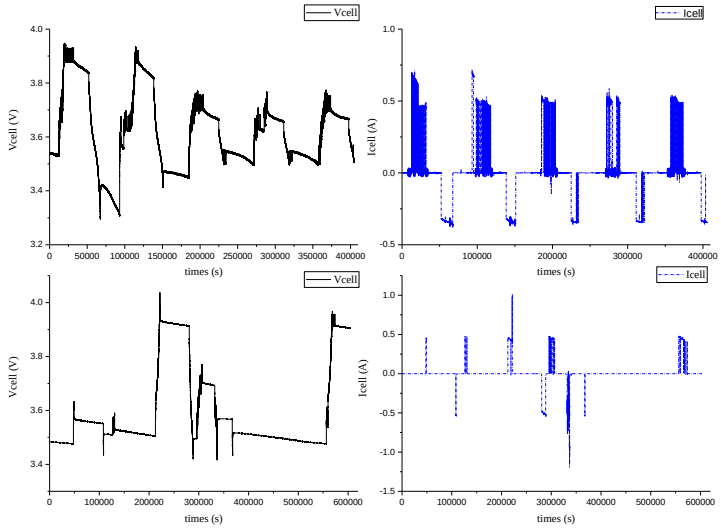


**Figure 2-5 Current and voltage profile for Test B, Test C Application Sites**

### 2.4.3. Sensitivity Analysis for Model Parameter

Based on DC-IR data and CPPT data, battery model parameters in various degradation states, SOC, temperature, and current can be obtained. The estimated parameters can be designed as lookup tables and used as the lower and upper bounds of the parameter constraints for observer design or SOH estimation.

Evaluation of the SOH model is carried out basically in two parts. One part is to evaluate how error difference is large between measured voltage and model voltage, and the other is to examine whether the model voltage patterns reflect polarization phenomena in the model circuit. The error minimization is effectively achieved by optimizing the parameter estimations for the objective function, which produce estimated voltages implicitly describing the polarization effects.

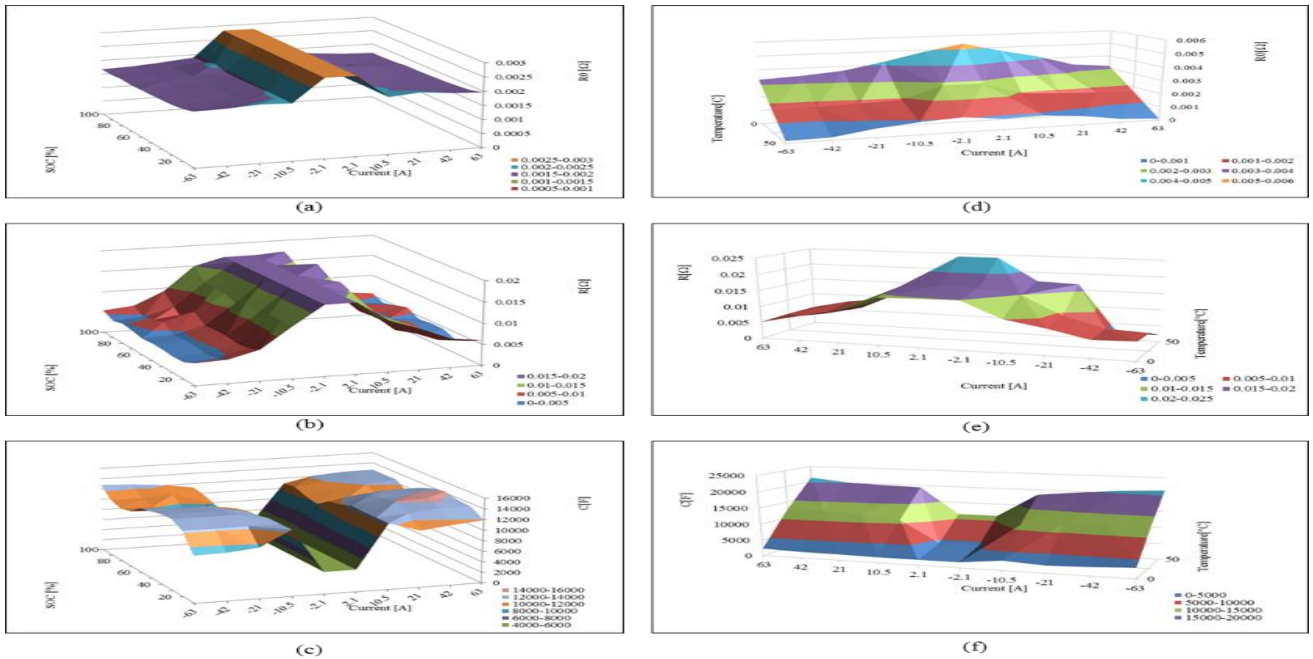


**Figure 2-6　Battery parameters trends under various experimental condition (a) SOC(%) vs. Current(A) vs.$R_0(\Omega)$, (b) SOC(%) vs. Current(A) vs. R(Ω), (c) SOC(%) vs. Current(A) vs. C(F), (d) Temperature(℃) vs. Current(A) vs. $R_0(\Omega)$, (e) Temperature(℃) vs. Current(A) vs. R(Ω), (f) Temperature(℃) vs. Current(A) vs. C(F).**

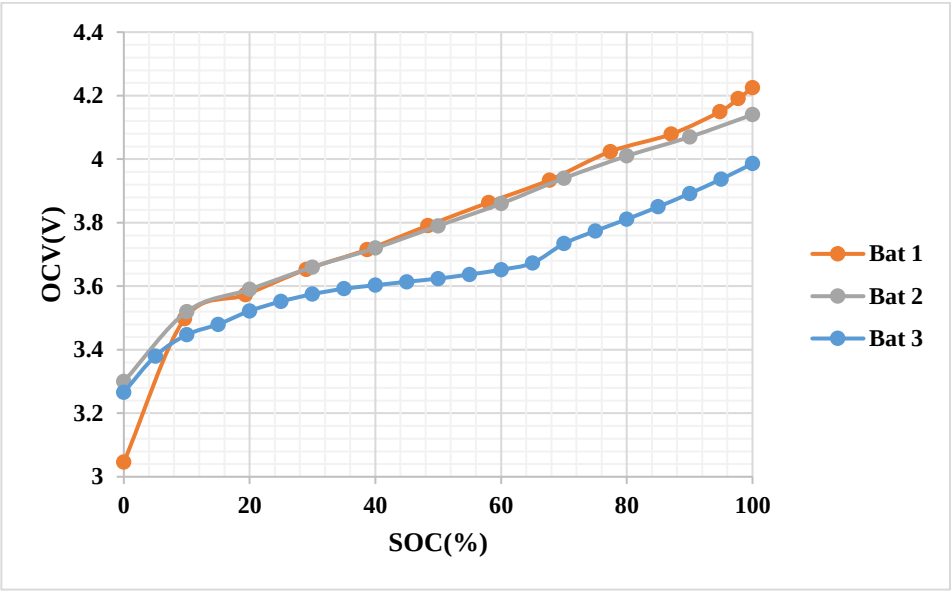


**Figure 2-7 SOC-OCV curve about 3 Batteries(Bat 1(NCM+LMO/GP+GC), Bat 2(NCM+LMO/LFP), Bat 3 (LMO/GC))**

Figure 2-7 shows battery parameters trends under various experimental condition. These results are summarized in Table 2-5. Battery internal resistance, R0, is primarily changed by temperature and current amount. Based on the battery test results with each degradation cycle in terms of temperature, SOC, and current, it was found that SOC variations remain mostly unchanged while R0 is highly increased in a low temperature condition. This pattern shows that the mobility of Li+ ion is diminished by the increase of electrolyte resistance, which leads to the decrease of overall electron conductivity. Interestingly, the values of R0 are rather increased in a high temperature than those of it in a room temperature for 700 cycled degradations, involved in high C-rate. This behavior may possibly indicate that the decomposition of electrolyte originated in the condition mentioned above draws to the increases of R0 values. In the case of R and C values which describe polarization phenomena at electric double layers, it was ensured in this study that the parameter values are largely changed by current amount and SOC variations. R value displays the decreasing trend as ambient temperature is increased, and this trend clearly appears in the condition where high currents flow into the battery. In regarding SOC, the trend of R shows more definite decreases as SOC is increased. For C trend, it is increased as temperature is increased, but SOC does not have any effect on C patterns.

**Table 2-5 Summary of the battery parameters affected by ambiente condition variables.**

| Parameter | Temperature conditions | | |
|---|---|---|---|
| | **Temperature (K)** | **SOC (%)** | **Current (A)** |
| $OCV$ | Negligible | Changes | No effects |
| $R_0$ | Changes | Negligible | High in low current |
| $R, C$ | Changes | $R$ changes | Changes by current amount |

## 2.5. Result and Discussion

The estimation accuracy of the model voltage for each test battery was compared to verify the SOH algorithm. In addition, the accuracy of the SOH algorithm was verified for each test battery.

### 2.5.1. Estimation results of battery model

Battery 1, 2, and 3 were analyzed for the model. Based on this, it is confirmed that the equivalent circuit model parameters are well estimated and the battery voltage can be adjusted relatively accurately. Based on this model parameter, it is utilized in the nonlinear system of observer. The average error rate of the battery 1 and 3 model voltages is about 1.3% and the maximum error rate is 2.13%.

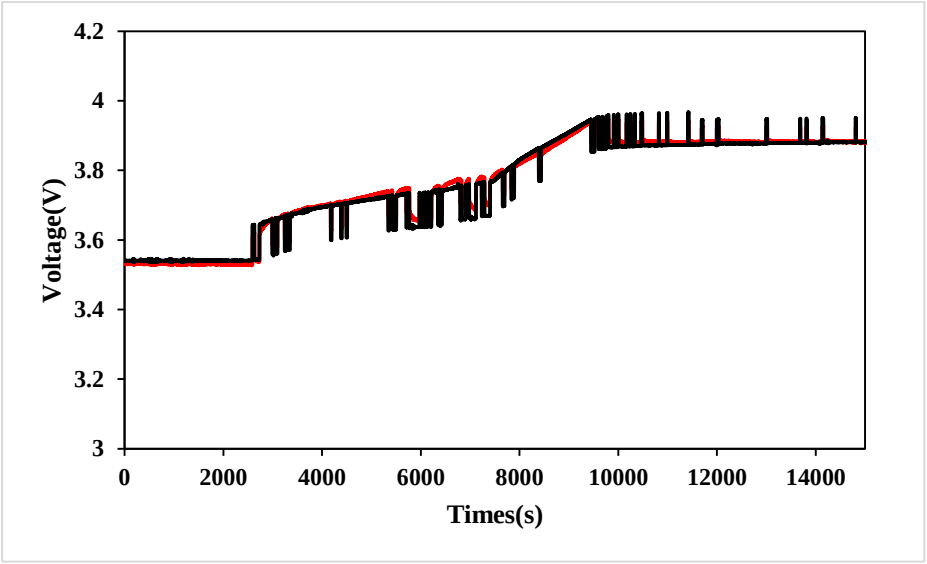


**Figure 2-8 Validation of the battery model and parameter estimation for Bat 1**

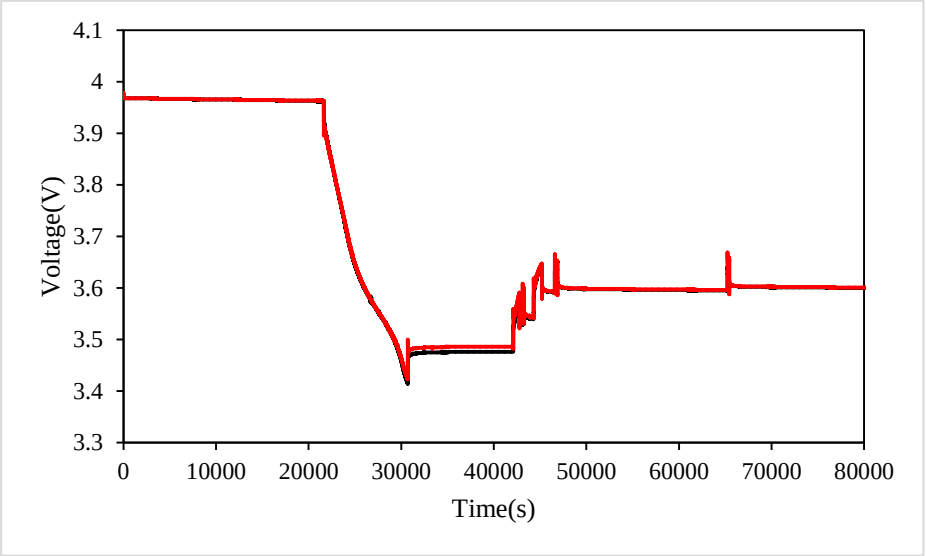


**Figure 2-9 Validation of the battery model and parameter estimation for Bat 2**

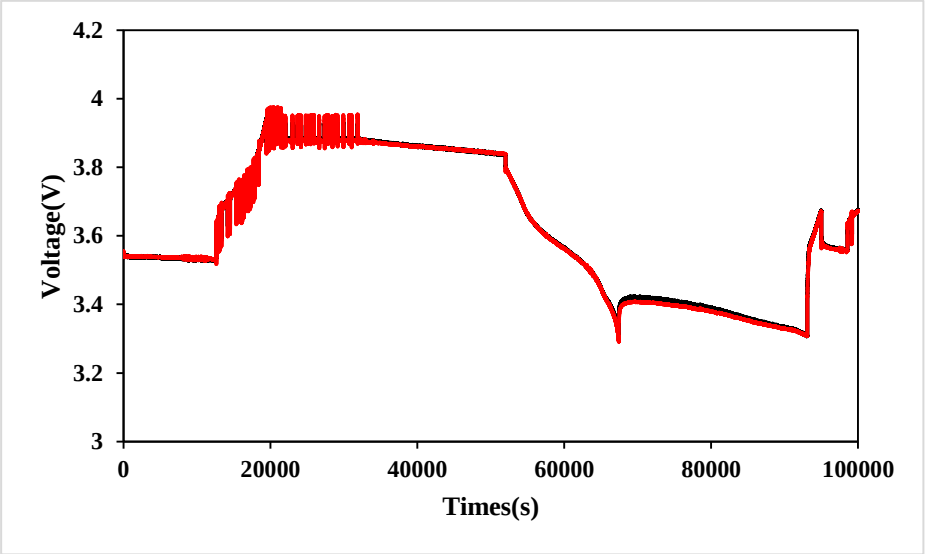


**Figure 2-10 Validation of the battery model and parameter estimation for Bat 3**

### 2.5.2. Estimation results of proposed method

Based on the proposed methodology, SOH estimation is performed. The test cases and the capacity fade values for the batteries 1, 2, and 3 were obtained by calculating the installation year and the forced deterioration conditions, respectively. The estimation results were obtained based on the test operation data obtained for each cycle. It is confirmed that the proposed method can compensate the chattering phenomenon that may occur in the battery model voltage and predict SOH with higher accuracy.

Next, we compare the proposed method with degradation cell capacity value. The proposed algorithms are also possible with maximum error rate within 3%. In the proposed method, we confirmed that the average error rate of about 1.9% can be secured.

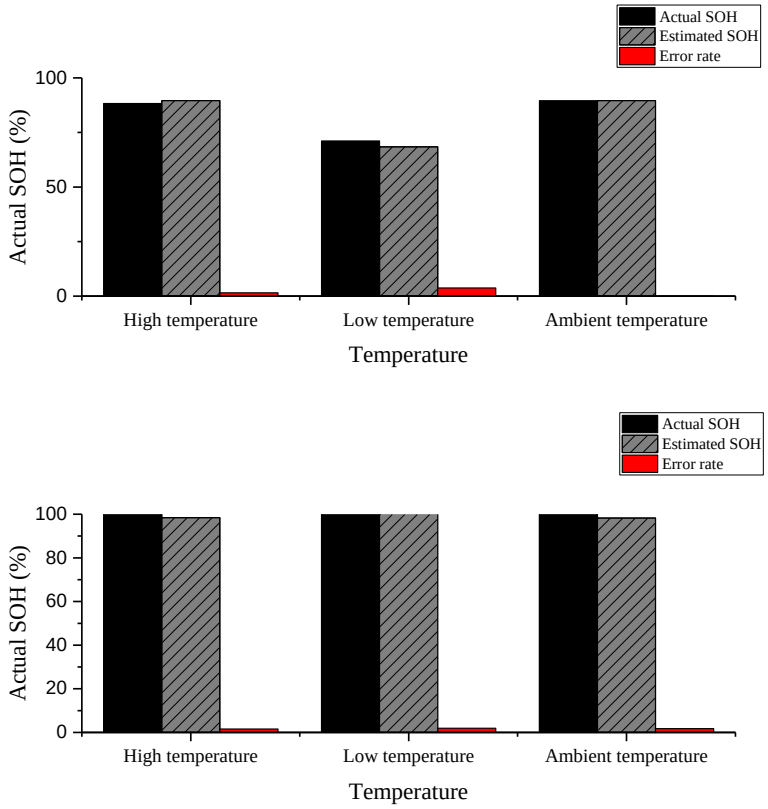


**Figure 2-11 Capacity Degradation Cycle Data(High Temperature 50℃, Ambient Temperature 25℃, Low Temperature 0℃)**

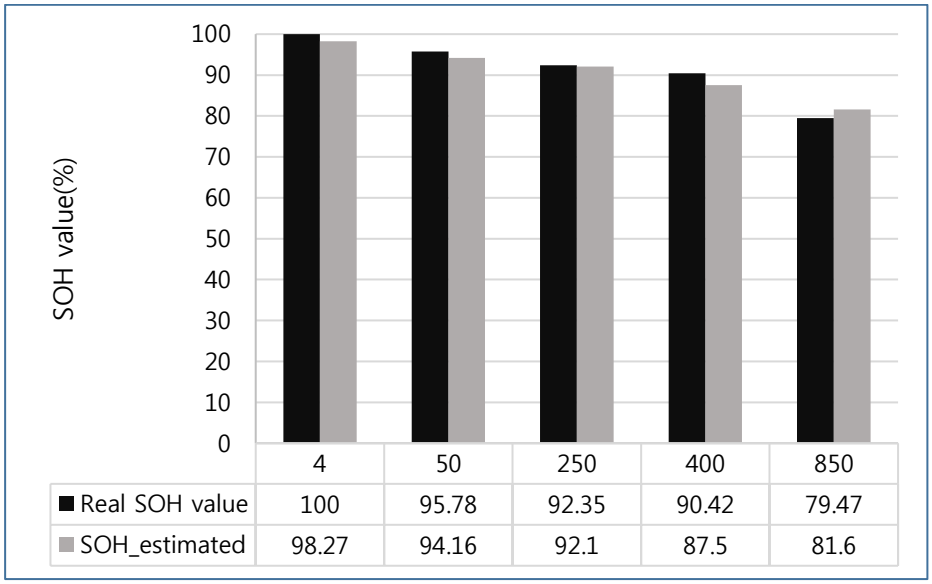


**Figure 2-12 The Proposed algorithm Estimation Result each degradation cycle(Cell data)**

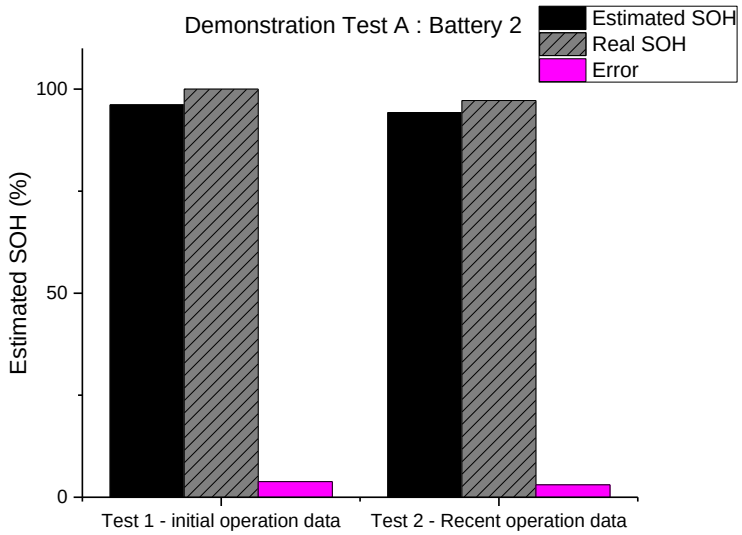


**Figure 2-13 Comparative SOH estimation result about ESS cell battery (Bat 2)**

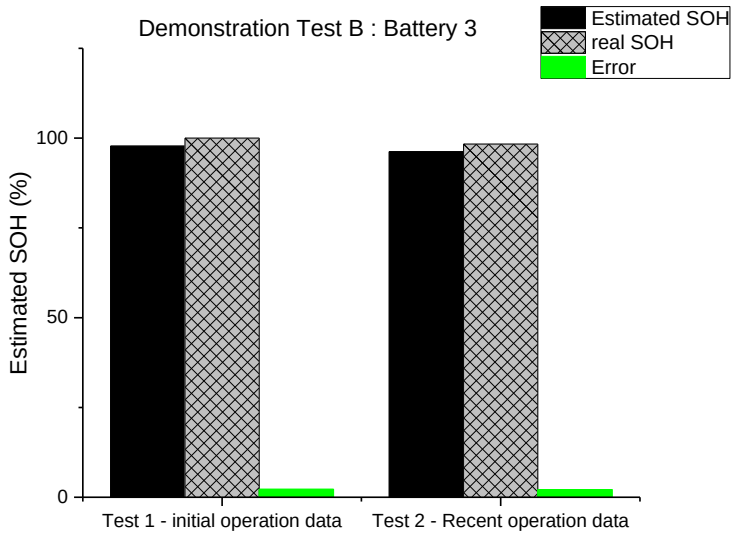


**Figure 2-14 Comparative SOH estimation result about ESS cell battery (Bat 3)**

## 2.6. Conclusion

SOH can be measured by Capacity fade and Resistance Fade, but direct measurement by EIS consumes considerable labor and cost. In addition, as applications in increasingly isolated systems and environments are increasing, equipment with high durability is being developed without immediate maintenance.

In order to develop the SOH estimation algorithm for the lithium ion battery which is popularized in the whole industry, the methodology is implemented based on the observer technique and parameter estimation method. Since the proposed algorithm operates separately from the internal BMS, it is easy to apply in various ESS environments. For this purpose, the system factor was introduced to calibrate the battery operation voltage to about 3.0V-4.3V, and the algorithm was configured to be able to estimate with various operation voltage and current data. Based on the EKF, the SOC uses a more accurate filtering technique than the current integration method, and the SOH is predicted from the capacity estimation through Adaptive Parameter Optimization suitable for ESS daily operation. Test data set comparison showed high accuracy of about 1-3%.

# CHAPTER 3. Reliability estimation modeling for quantitative risk assessment about underground pipeline

## 3.1. Introduction

Pipeline systems, which is a typical fluid transport method, is managed by industrial companies. However, there have been fatalities in the world due to the explosion of gas pipeline in Kaohsiung, San Bruno and Ghislenghien pipeline leakage and pipe breakage accidents. Many accidents have been caused by defects in the welds, pipe breakage due to construction work, and the lack of proper piping management in accident reports. Most of the buried pipelines are not appropriately managed due to difficulties in management and investment of safety expenses. Various methods for efficiently managing buried pipelines have been attempted.[40]

Quantitative risk assessment is a methodology that helps determine how various risk reduction measures in the risk assessment field can be reasonably implemented in accordance with ALARP decisions. Many quantitative risk assessments use risk assessment methodologies based on accident history and often follow criteria set by field experts in the field or decades of experience. Fuzzy logic, Structural Reliability Analysis, and Probabilistic Approach can be considered as a method to consider this because many safety problems have uncertainties. Especially, safety management of buried piping has an

indeterminate factor related to the reliability and accuracy of inspection data. There is a clear contradiction between the safety measures that reduce risk and the economy. In other words, a lot of safety measures will increase safety and reduce accidents, but the costs will rise accordingly On the other hand, if safety measures are insufficient, the investment cost is reduced but the risk of accidents increases. A systematic framework is needed to make decisions about safety management considering both risk and economy.

**Table 3-1** Domestic and overseas buried pipeline accidents

| Domestic (Korea) | | | | |
|---|---|---|---|---|
| Region | Accident Date | Failure cause | Fluid | Installation year |
| Ulsan | 2014.1 | Equipment Impact (Welding joint failure) | Propane, Oil | 1986 |
| Hwansung | 2010.5 | Equipment Impact (Drilling machine) | SiH4, N2 | 1990 |
| Ulsan | 2002.2 | External Corrosion | NH3 | 1979 |
| Yeosu | 2001.8 | External Corrosion (Connector defect) | Cl2 | 1980 |
| **Overseas** | | | | |
| Region | Accident Date | Failure cause | Fluid | Installation year |
| Kaohsiung, Taiwan | 2014.8 | External Corrosion | Propylene | 1990 |
| Kingman, USA | 2004.1 | Metal fatigue crack | NH3 | 1973 |
| SanBruno, USA | 2010.9 | Weld crack | Natural gas | 1956 |
| Westcoast, Canada | 2012.6 | Wild fire breakage | sour gas | 1985 |

## 3.2. Uncertainties in underground pipeline system

Underground pipeline systems have large numbers of uncertain or random variables such as pipe geometry, material properties, corrosion threats, and equipment impact factors. The difficulties in predicting pipe reliability are as follows. (1) setting the limit state function for pipe failure composed of random variables, (2) setting the appropriate probability distribution model and parameter value for each random variable, (3) Verification of settings and results for rare pipeline accident scenarios (4) Considering modeling error, (5) Insufficient data for underground piping model construction.

Buried pipeline systems are characterized by a large number of degrees of freedom, time-varying and response dependent nonlinear behavior. In the presence of uncertainty in this system, performance of an underground pipeline can be considered using ‘performance margin’ or ‘safety margin’. Through predicting the pipeline reliability, the safe service life can be estimated with a view to prevent unexpected failure of underground pipelines by prioritizing maintenance based on failure severity and system reliability.[41, 42]

The parts for (1) and (2) can be used by defining the limit state function and probability model for each cause of accident presented in CSA Z662-07, BS EN ISO 16708-2006, ASME B 31.8 Code verified from numerous experiments . (3) It is possible to verify the approximate result based on the comparison of the accident probability predicted by the pipe reliability model constructed with

the actual accident history. EGIG, PHMSA, OGP etc. Pipeline incident historical data. (4) and (5) can be supplemented by introducing a modeling error term into the pipe resistance model.

## 3.3. Probabilistic based Quantitative Risk Assessment Model

### 3.3.1. Structural Reliability Assessment

SRA(Structural Reliability Analysis) quantifies a structure's reliability by accounting explicitly for uncertainties in parameters that control integrity. This method is different from other methods because it makes these explicit by using statistics and then finds their effect. SRA quantifies reliability by applying standard probability methods to assess the contribution from each source of uncertainty. This method has several benefits as follows.

- Investigating several mitigation options for reducing risk based on sum of expected failure cost and maintenance cost

- Ensuring that the calculated confidence of the system to which the mitigation action is applied is higher than the target reliability

- Applicable for inefficient and highly uncertain system because of probabilistic approach

Figure 3-1 shows the general pipe failure rate with time as “Bathtub curve”, which is widely used in reliability engineering. It describes the overall network’s failure rate changing with time. This failure function comprises of three parts “early failure period”, “intrinsic failure period”, “Wear-out failure period”. This paper does not consider the change of reliability for the early failure period because it addresses the problem of aging underground pipeline management optimization.

Intrinsic failure period is known as random failure such as equipment impact and pipeline is operated relatively trouble free with low failure frequency level. Wear-out failure period shows that failure frequency is increasing due to degradation of the pipe material which finally leads to the leakage or rupture of the pipe. The bath-tube curve explains the failure probability during pipeline’s whole service time without any pipe rehabilitation. Therefore, reliable pipeline management should be considered rehabilitation effects.

The total annualized cost is consists of the expected failure cost and maintenance cost. Both costs are quantified based on the implicit probability calculation model, the accident prediction model, and the rehabilitation logic.The main purpose of the RIMAP (Risk Based Inspection and Maintenance for European Industries) used in Europe is to determine the priority of risk remediation activities as a risk value calculated as the combination of probability and consequence of failure. In calculating the risk, the PoF is

calculated in the same way as Statistical models based on generic data, fuzzy approach, and structural reliability models with Bayesian approach..Then this methodology can find an optimal management method according to each maintenance methodology by performing cost-benefit analysis for the scheduled maintenance scenario.

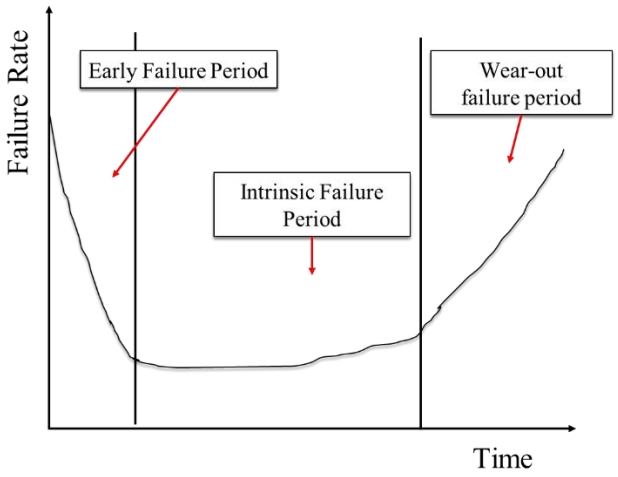


**Figure 3-1** Bathtub curve for pipe failure

### 3.3.2. Failure mode

In order to construct a quantitative risk assessment model based on probability theory, it is necessary to establish a limit state function that can analyze the piping accident situation. According to CSA Z662-07 Oil and Gas pipeline Systems, failure probability $\lambda_f$ can be calculated as

$$\lambda_f = \omega \times p_f \quad (37)$$

Where $\omega$ is the frequency of failure occurrence event, $p_f$ is the conditional probability of failure given an occurrence of the event. Pipeline reliability calculation should be considered time variability. It is classified as either time-dependent or as time independent. The probability of failure during a specific time can be calculated using cumulative probability distribution of the using $F_t(\tau)$. [43] Annual probability of failure at specific time is calculated when the $\tau_1$=0.

$$F_t(\tau) = \mathrm{p}[g(x) = R(\tau) - S(\tau) < 0] \quad (38)$$

$$p_f(\tau_1, \tau_2) = \mathrm{p}(\tau) = \frac{F_t(\tau_2) - F_t(\tau_1)}{1 - F_t(\tau_1)} \quad (39)$$

According to the European Gas Pipeline Incident Data group(EGIG) Report, the major Pipeline incident causes during 2009-2013 are External Interference and Corrosion. The causes of Incident were 28% External Interference and 26% Corrosion. Therefore these two failure threats are selected pipeline failure main causes.

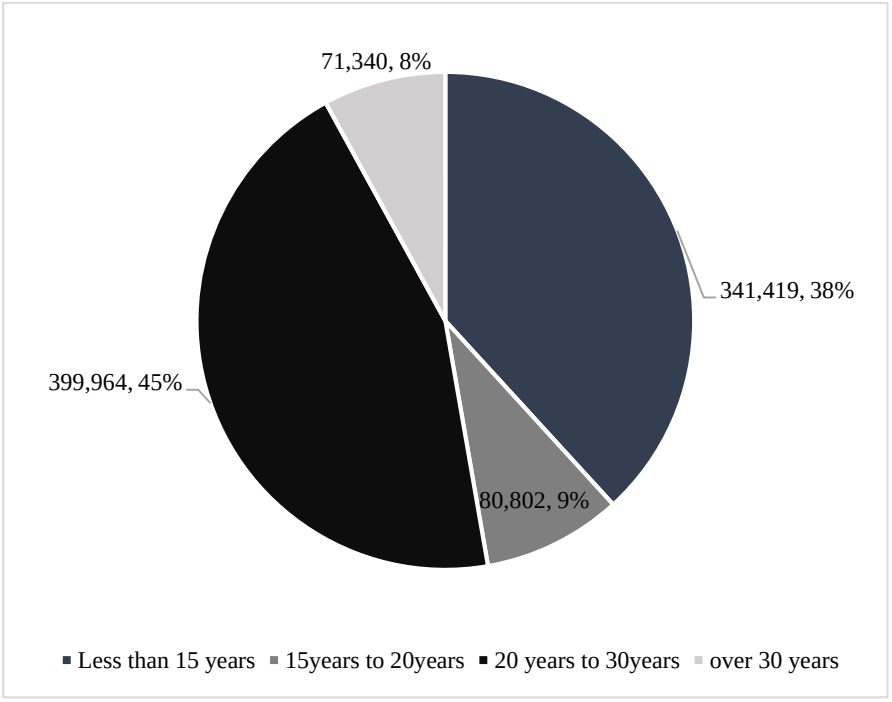


**Figure 3-2. Burial period of domestic Industrial complex underground pipeline**

ω is corresponded to the Hit frequency in the time-dependent element, External Interference, and depends on one-call system or patrol. On the other hand, External Corrosion, which is a time-dependent cause, corresponds to defect density. The actual number of corrosion defects of the target pipe can be confirmed through indirect inspection and excavation of the pipeline, but inspection of the entire pipeline is impractical in terms of cost. Therefore, this study set the appropriate defect number growth rate based on inspection historical data and introduced a linear defect growth model.

Failure mode is divided into small leak, large leak, and rupture. In CSA Z662 Standard and British Gas, each failure mode and hole size are defined as follows

Small leak : occurs if the maximum defect depth exceeds the wall thickness.(absolute hole size : 10mm)

Large leak : occurs if the internal pressure exceeds the burst resistance at the corrosion defect. it is related to both defect depth and length(large leak : 50mm)

Rupture : burst of a corrosion defect results initially in a leak. If the length of the resulting breach is large enough, unstable axial growth could occur leading to a rupture(rupture : Pipe Diameter)

Failure mode is divided into small leak, large leak, and rupture. Limit states are defined as below table. When failure rate is calculated in each failure mode, it is possible to calculate the total failure probability based on this. The elements

constituting each limit state function are composed of line attribute, pipe resistance, model error factor, and defect attributes. Corrosion is determined as $g_{2,3}$ when distinguishing between large leak and rupture from pipe body failure, which is a large leak occurs if $g_{2,3} < 0$ and a rupture occurs if $g_{2,3} > 0$. Following equation can estimate the overall failure rate and probability by integrating the failure rate for each failure cause and mode.

$$p_{i,j} = \mathrm{p}[g_{i,j} < 0] \quad (40)$$

$$p_i = 1 - \prod_{j=1}^{3}(1 - p_{i,j}) \quad (41)$$

$$p_{total} = 1 - \sum_{i=1}^{i=2} \omega_i \, p_i \quad (42)$$

($\mathrm{i} = 1; \text{Equipment Impact},\ \mathrm{i} = 2; \text{Corrosion}, \mathrm{j} = 1; \text{smll leak}, \mathrm{j} = 2; \text{large leak}, \mathrm{j} = 3; \text{rupture}$)

### 3.3.3. Limit state function and variables

The most important variables in the calculation of the limit state function related to corrosion are defect depth and length. As these two defect attributes grow to a certain size, the pipe resistance decreases and the failure rate gradually increases. Defect size model was selected as follows. In general, $d_{avg}$ has a linear growth model assuming that the growth rate is constant according to the external corrosion environment condition at the time before maintenance action.

However, the growth rate is not constant because there is an update to the corrosion situation after the maintenance action. Through the maintenance action, the defect population changes toward the direction of decreasing the defect population based on the defect critical size, thus affecting the failure rate. To reflect this in the limit state function, we assume the function of the time of the defect depth for the time after the maintenance action as the exponential equation. Kiefner and Vieth 1989[44] found that there is a linear correlation between the maximum defect depth and the average defect depth, and the coefficient is 2.082, with a mean shifted lognormal distribution of 1.063.

$$\begin{cases} d_{avg}(\tau) = g_{davg}(\tau + \tau_{l0})^{n_{davg}} \ (\tau > \tau_{maintenance}) \\ d_{avg}(\tau) = d_{avg0} + g_{davg0}\tau \ (\tau < \tau_{maintenance}) \end{cases} \quad (43)$$

$$d_{max}(\tau) = c d_{avg}(\tau) \quad (44)$$

where t is time elapsed since interested time, $h_{avg}(\tau)$is the average defect depth at time $\tau$, $g_{davg}$ is an average depth grwoth rate constant, $n_{davg}$ is the time exponent for the depth growth rate, $\tau_{davg0}$ is a depth growth time delay constant, $d_{max}(\tau)$is the average defect depth at time $\tau$, c is defect depth correlation parameter. Thus, the defect length is also expressed.

$$\begin{cases} \mathrm{l}(\tau) = g_l(\tau + \tau_{l0})^{n_l} \ (\tau > \tau_{maintenance}) \\ \mathrm{l}(\tau) = l_0 + g_{l0}\tau \ (\tau < \tau_{maintenance}) \end{cases} \quad (45)$$

$l(\tau)$ is maximum axial defect length at time $\tau$, $g_l$ is a length growth rate at time of interested time, $\tau_{l0}$ is a length growth time delay constant, $n_l$ is the time exponent for length growth rate, $g_{l0}$ is the length growth rate at the time prior maintenance action.

Including in $g_{1,1}$ $g_{2,3}$ actual pipe resistance as a function of time can be expressed as

$$r_a = \frac{c_1 2.3ts}{d}\left\{\frac{1-\frac{g_{davg}\left(\tau+\tau_{davg0}\right)^{n_{davg}}}{t}}{1-\frac{g_{davg}\left(\tau+\tau_{davg0}\right)^{n_{davg}}}{m(t)t}}\right\} + \frac{2.3ts}{d}(1-c_1) - c_2 s(\text{Corrosion}) \quad (46)$$

Where t is wall thickness, S is the yield strength, $c_1$ is the multiplicative model error factor, $c_2$is the additive model factor and m is the Folias factor.

The pipe resistance calculation for Equipment Impact is as follows. This equation was verified as experimental data in Muntiga 1992, Hopkins 1992, Chatain 1993.

Also, This model is calibrated for values of t between 4 and 12.5mm, d between 168-914mm, yield strength up to 483Mpa.

$$r_a = [1.17 - 0.0029\frac{d}{t}]\frac{(l_t+w_t)ts}{1000} + e \quad \text{(Equipment Impact)} \quad (47)$$

Where $l_t$the cross-sectional length of the indentor, $w_t$ is the cross-sectional width of the indentor, e is model error term.

Normal impact force q of Equipment Impact can be calculated as

$$\mathrm{q} = 16.5\, w^{0.6919}\, R_D R_N \quad (48)$$

where w is the excavator mass(tonne), $R_D$ is the dynamic impact factor, 2/3, $R_N$ is the normal load factor,

The limit state function for dent gouge failure $g_{1,2}$ is presented below. $g_{1,2}$ is consists of ERPG semi empirical model about Linkens Model[44] and Francis[45]. This model has a conservative assumption that all gouge defects have axial orientation. Critical hoop stress, $\sigma_c$ and hoop stress, $\sigma_h$ equation is as follow

$$\sigma_c = \frac{2}{\pi b_2} arccos\left[exp\left\{-125\pi^2 \left(\frac{b_2}{b_1}\right)^2 \frac{{K_{IC}}^2}{\pi d_g}\right\}\right] \quad (49)$$

$$\sigma_h = \frac{pd}{2t} \quad (50)$$

Where $K_{lc}$ is the critical stress intensity, m is the folias factor, $d_g$ is the gouge depth, b1 and b2 are parameter which is the function of dent depth, Folias factor and gouge length.

Equipment rupture is determined based on whether or not unstable axial growth of the resulting through wall defect occurs. Given limit state function

of $g_{1,3}$ is developed by Kiefner.[44] Critical pipeline rupture resistance $S_{cr}$ can be calculated as follows

$$S_{cr} = \frac{2(s+68.95)}{\pi M_t} cos^{-1}\left[exp - \left\{\frac{125\pi EC_v}{c(s+68.95)^2 A_c}\right\}\right] \quad (51)$$

$A_c$ is the ligament of full size Charpy specimens, $C_v$ is the full size Charpy V notch palteau energy, E is the elastic modulus, c is the one-half the defect length. The probabilistic model for the various piping variables used in the calculation of the accident probability of the above limit state function is summarized in the table.

**Table 3-2 Limit state functions for each failure mode**

| Failure cause, i | Failure mode, j | Limit State function, $g_{i,j}$ | Description |
|---|---|---|---|
| Equipment Impact -puncture,1 | Small leak, 1 | $g_{1,1}: r_a - q$ | $r_a$:estimated resistance(impact)<br>q: normal impact force |
| External Corrosion,2 | Small leak. 1 | $g_{2,1}: t - d_{max}$ | $t$ : wall Thickness<br>$d_{max}$ : maximum corrosion depth |
| Equipment Impact,1 | Large leak, 2 | $g_{1,2}\ \sigma_c - \sigma_h$ | $\sigma_c$ : critical hoop stress<br>$\sigma_h$ : hoop stress |
| External Corrosion,2 | Large leak, 2 | $g_{2,2}: r_a - P$ | $r_a$ : estimated resistance (corrosion) |
| Equipment Impact,1 | Rupture, 3 | $g_{1,3}: S_{cr} - \sigma_h$ | $S_{cr}$ : critical resistance with unstable axial defect growth |
| External Corrosion,2 | Rupture, 3 | $g_{2,3}: \frac{pD}{2ts} - \frac{115}{m}$ | m : folias factor<br>$\sigma_u$ : tensile strength |

**Table 3-3 Input variable probability distribution for pipeline structural reliability assessment**

| Classification | Variables | Distribution Type | Mean | COV(%) | Reference |
|---|---|---|---|---|---|
| Pipe mechanical Structure | Diameter | Normal | 1 | 0.06 | Zimmerman et al. (1998) |
| | Wall Thickness | Normal | 1 | 0.25/nominal | Jiao et al (1997) |
| Pipe mechanical Property | Yield Strength | Normal | 1.11 | 3.4 | Jiao et al (1995) |
| | Tensile Strength | Lognormal | 1.12 | 3 | Jiao et al (1997) |
| | Charpy-V-notch Energy | Lognormal | 204 | 21 | Jiao et al (1995) |
| | Youngs-Modulus | normal | 210 | 4 | CSA Z662-07 |
| Load(Equipment Impact) | Excavator Weight | Beta | 5.7 | 8 | Wolvert et al(2004) |
| Load(Defect attributes) | Corrosion length | lognormal | 27 | 35 | Proprietary data(CSA Z662-07) |
| | Corrosion Depth | Weibull | 0.2 | 30 | Proprietary data(CSA Z662-07) |
| | Max / Avg Defect depth ratio | Shifted Lognormal | 2.08 | 50 | Kiefner and Vieth (1989) |
| | Dent depth | weibull | 13 | 95 | ISO 16708 |
| | Gouge depth | weibull | 1.2 | 92 | Jiao et al |
| | Gouge length | weibull | 153 | 125 | Wattis and Noble (1998) |

### 3.3.4. Reliability Target

Reliability target express the minimum acceptance criteria required to ensure adequate pipeline safety. The methodology for derivation of adequate reliability target is from the Gas Research Institute report. CSA Z662-07 defined Ultimate Limit Sate. And target reliability level calibrated to a series of pipeline designs based on ASME B31.8 using design parameters and operating condition intended to be representative of Korea Industrial Complex. [46] Gas Research Institute calibrates of societal risk level for establishing reliability target which represents the minimum criteria required to ensure adequate safety. [47] The reliability target for ULS were developed using a risk based approach that ensures consistent and reasonable safety levels for all pipelines. Generally, ULS reliability target is defined as an increasing function of pipeline diameter(D), pressure(P), and population density. This targets are based on tolerable risk criteria such as societal risk or individual risk. The societal risk are intended to limit risk exposure to all members of society due to all pipeline accident. In this this research, target is based on a consequence model that has been developed and validated for lean natural gas only. This thesis treat Ethylene, Propylene, Butadiene, n-Butane, Hydrogen, Nitrogen, Oxygen, Carbon dioxide, Ammonia as additional product working fluids.

$$p_{max} = \frac{r_{max}}{c} \quad (52)$$

$$R_T = 1 - p_{max} = 1 - r_{max}/c \quad (53)$$

$R_T$ is defined as the annual probability that the pipeline will not fail, $p_{max}$ is maximum permissible failure rate, c is failure consequences. $r_{max}$ is the tolerable level of risk. The development of $R_T$ requires an appropriate consequence model and an acceptable set of tolerable risk criteria.

C is calculated according to the potential impact radius equation depending on the flammability and toxicity type of the material.

$$c = p_i \rho \tau \pi \left[ P_{in} \left( 0.25 ({r_{1\%}}^2 - {r_{100\%}}^2) \right) + P_{out} \left( 0.5 ({r_{1\%}}^2 - {r_{100\%}}^2) \right) + {r_{100\%}}^2 \right] \quad (54)$$

$P_{in}$ is proportions of time spend indoor, 0.9, $P_{out}$ is proportions of time spent outdoor, 0.1, $p_i$ is ignition probability, $\tau$ is occupancy probability, 0.4.

Maximum tolerable individual risk criteria used in this work were selected based on information published by HSE(2001) and MIACC(1995). Annual tolerable risk levels of $10^{-4}$ in class 1, $10^{-5}$ in class 2, and $10^{-6}$ in class 3 and 4. Pressure range is 20, 30, 40, 50, 60 bar, and Pipe diameter range is 50mm-300mm, population density is 0.00001-0.01 number/$m^2$

The calculated reliability target at each pipeline condition is fitted below equation.

$$R_T = 1 - \frac{A_1}{(\rho P D^3)^{A_2}} \quad (55)$$

**Table 3-4 Summary of Reliability target parameters (8 Products)**

| Product | Parameter | | | |
|---|---|---|---|---|
| Ethylene | A2 | 0.6294 | 0.7049 | 0.7218 |
| | A1 | 7.1042.E-08 | 2.9990.E-09 | 1.6004.E-09 |
| Propylene | A2 | 0.5125 | 0.4919 | 0.4883 |
| | A1 | 6.5777.E-08 | 4.8127.E-09 | 2.3286.E-09 |
| Butadiene | A2 | 0.4935 | 0.4572 | 0.4503 |
| | A1 | 7.4163.E-08 | 5.9255.E-09 | 2.8215.E-09 |
| N-butane | A2 | 0.4872 | 0.4458 | 0.4378 |
| | A1 | 2.15781E-07 | 1.77656E-08 | 8.4171E-09 |
| Hydrogen | A2 | 0.6552 | 0.752 | 0.7734 |
| | A1 | 1.0011E-07 | 3.74067E-09 | 2.03861E-09 |
| Nitrogen | A2 | 0.662 | 0.853 | 0.8841 |
| | A1 | 7.38544E-06 | 1.20695E-07 | 6.8942E-08 |
| Oxygen | A2 | 0.5015 | 0.474 | 0.4687 |
| | A1 | 2.93858E-05 | 2.21779E-06 | 1.06451E-06 |
| Carbon Dioxide | A2 | 0.3683 | 0.3197 | 0.2996 |
| | A1 | 0.001341187 | 8.79537E-05 | 3.93112E-05 |
| Ammonia | A2 | 0.3098 | 0.1223 | 0.0833 |
| | A1 | 4.15998E-06 | 7.88605E-07 | 3.21908E-07 |

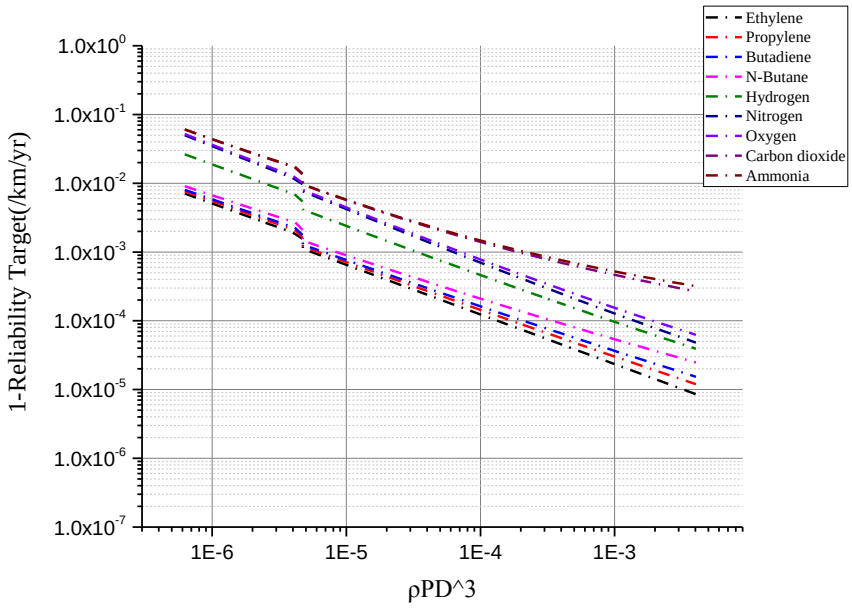


**Figure 3-3 Reliability Target as a function of population density based on Societal Risk**

### 3.3.5. Failure frequency modeling

Failure frequency is the factor that determines the failure probability along with the failure rate. This element is divided into two parts according to the failure cause. There are Hit frequency related to equipment impact and corrosion defect density related to external corrosion

Corrosion growth rate model is used to estimate the corrosion density. Historical ECDA data from buried piping were used to select modeling parameters. The data are based on the Korea Gas Safety Corporation 's Pipeline Safety Diagnosis Report and Ulsan Industrial Complex Industrial Service Performance Results. Indirect corrosion tests show that if all of the suspected defects are actually excavated, it is possible to identify the actual corrosion defects, but the conditions for the complex buried excavation could not be secured. Therefore, within the observation data, damage spot which is Ⅳ or more according to the risk assessment standard is determined as a defect through NACE standard SP0502 among the coverage damage probes detected by the DCVG method. These data were used as annual defect accumulation rate and initial defect density conditions.[48]

$$\rho_{a,t} = \rho_{a,i} + \gamma \cdot t \quad (56)$$

$\rho_{a,t}$ is actual defect density at time t, $\gamma$ is subsequent defect accumulation rate. $\rho_{a,i}$ is guaranteed defect density at inspection year.

$$\rho_{a,i} = \frac{\rho_{d,i}(1-p_{fi})}{p_d} \quad (57)$$

$\rho_{a,i}$ is actual defect density, $p_d$ is probability of detecting a randomly selected defect, $\rho_{d,i}$ is measure density of detected defects $p_{fi}$ is probability that a given defect indication is false. $p_d$ is related inspection method accuracy.

**Table 3-5 Basic Event frequency of Pipeline Fault tree model**

| Basic Event | Input Variable | Probability Definition | Condition | Frequency |
|---|---|---|---|---|
| B1 | Excavation on pipeline alignment | Frequency of excavations on pipeline alignment | A. Ulsan Industrial Complex, Korea | 1.8086 |
| B2 | Third party unware of one-call system | Probability that a third party is not aware of one-call system | A. Community meeting (Ulsan) | 0.1 |
| B3 | Right of way signs not recognized | Probability that a third party fails recognize ROW signs | A. Intersection Marker<br>B. All Intersection point<br>C. Linemark | A. 0.23<br>B. 0.19<br>C.0.17 |
| B4 | Failure of permanent markers | Probability that permanent markers are not recognized | A. No patrol / Marker<br>B. Patrol / Marker<br>C. Patrol / Linemark | A. 0.1<br>B. 0.05<br>C. 0.02 |
| B5 | Third party chooses not to notify | Probability that a third party is aware of one-call or ROW signs but chooses not to notify | A. No notification<br>B. Notification | A. 0.1<br>B. 0.33 |
| B6 | Third party fails to avoid pipeline | Probability that a third party fails to avoid pipeline, given that the party is aware of one-call or the existence of the pipeline but chooses not to notify | Not to notify | 0.4 |

| | | | | |
|---|---|---|---|---|
| **B7** | **ROW patrols fail to detect activity** | **Probability that an unnotified excavation is not detected by employee** | **Daily Patrols** | **0.3** |
| **B8** | **Activity not detected by other employees** | **Probability that an unnotifed excavation is not detected by employees other tan patrol crew** | **Industrial Complex Characteristic** | **1** |
| **B9** | **Excavation prior to operator's response** | **Probability that a third party after notify of the activity, excavates before the pipeline is located and marked** | **Immediate response** | **0.02** |
| **B10** | **Temporary marker incorrect** | **Probability that a pipeline is not correctly located** | **By company record basis** | **0.2** |
| **B11** | **Accidental interference with marked alignment** | **Probability that excavation equipment accidentally interferes with a properly marked alignment** | **Onsite procedure for handling third party excavation** | **0.03** |
| **B12** | **Excavation depth exceeding cover depth** | **Probability that excavation depth exceeds cover depth** | **Cover depth 1.5m** | **0.07** |

The impact frequency model utilizes the fault-tree method. In the Fault tree model proposed by Q. Chen, 12 basic cases were adjusted to the Ulsan National Industrial Complex conditions in Korea.[49] This top event is composed of three input events and these events has AND relationship, since they must co-exist for the damage to occur.

Basic events representing the conditions that need to be satisfied for an impact to occur. Table 2 summarizes the 12 baseline events and the frequency that is matched to the Ulsan National Industrial Complex situation in Korea. In 2009-2017, the total observation length of Ulsan high pressure gas pipeline was 5,877km, the number of excavation works was 10,629, and the excavation frequency was 1.8 km per 1km · yr. In order to reflect the probability of discovery of excavation in the patrol period, daily patrol frequency value is applied because of that 56% of the companies perform daily patrol in the Ulsan area. In addition, this study used the frequency values to meet these conditions, reflecting the characteristics of the industrial complex and the status of the One-call system.

### 3.3.6. Consequence modeling

In order to quantify the risk for an Integrity action scenario as a cost, a predictive model of the accident scale is also needed. The consequence of failure is defined as the potential impact radius model and release rate model resulting from the pipeline failure at each failure mode. The magnitude of the failure dependent on pipeline attributes, location, hole size. [50]

The types of high pressure gas in industrial complex piping can be classified into flammable gas and toxic gas. For the accident modeling of high pressure gas, only the situation of Jet Fire and Toxic gas dispersion was considered. Jet fire is the most frequent accident type in plumbing fire accident.

Jet flame can be idealized as a series of point source heat emitters spread along the length of the flame. Total heat flux I at horizontal distance of r from the fire center is given by GRI Report.[50-52]

$$\mathrm{I} = \frac{\eta X_g Q_{eff} H_c}{4\pi r^2} \quad (58)$$

I is heat intensity, $\eta$ is efficiency factor, $X_g$is emissivity factor, radial heat fraction of the total heat $Q_{eff}$is effective release rate, $H_c$is heat of combustion, r is distance from the point of the accident to the victim.

The peak release rate, $Q_{in}$ from a single side of a guillotine line rupture can be estimated using gas discharge equation for sonic or choked flow through an

orifice. Assuming double-ended release at the failure of pipeline, effective release rate feeding a steady-state fire can be calculated as follows.

$$Q_{eff} = 2\lambda C_d \frac{\pi d^2}{4} \mathrm{p} \frac{\varphi}{a_0} (59)$$

λ release rate decay factor, $C_d$is discharge coefficient, d is effective hole diameter, p is pipeline pressure, $\varphi$ is flow factor, $a_0$ is sonic velocity of gas. The Potential Impact radius is derived from Eqs. 58 and 59 and is summarized as follows.

$$\mathrm{r} = \begin{cases} \left(\frac{14490 \cdot (0.75 \cdot 2.02 (P_w)^{-0.09} \cdot X_g \cdot \lambda \cdot C_d \cdot \varphi \cdot H_c \cdot p \cdot d^2}{a_0 \cdot I}\right)^{-2.09} (Flammable) \\ 2lnr + 0.0492(6.2 \cdot 10^{-4} P_w) r = \ln\left(\frac{14490 \cdot (0.75 \cdot 2.02 \cdot X_g \cdot \lambda \cdot C_d \cdot \varphi \cdot H_c \cdot p \cdot d^2}{a_0 \cdot I}\right) (Toxic) \end{cases}$$

(60)

The potential impact radius formula for each fluid are summarized equation (61).

$$\mathrm{r} = \begin{cases} A \cdot (p \cdot d^2)^B \\ A \cdot \ln(p \cdot d^2) + B \end{cases} (61)$$

r is potential impact radius, p is maximum operating pressure, d is the leakage hole diameter. Hole diameter size was calculated as 10 mm for small leak, (10 + pipe diameter/2 for large leak, and pipe diameter for rupture. The parameter values for the main materials are summarized for the pipelines in

Ulsan and Yeosu industrial complexes. The simplified potential impact radius formula was verified by Phast results, a commercial Consequence Analysis program. The error rate was around 2% in the range of pipe diameter 75mm ~ 300mm and operating pressure 20bar-70bar.

‘

**Table 3-6 . Parameters of Potential Impact Radius Equation**

**(5 Flammable fluids and 5 Toxic Fluids)**

| Type | Flammable | | Type | Toxic | |
|---|---|---|---|---|---|
| Product | Para A | Para B | Product | Para A | Para B |
| Ethylene | 108.4511 | 0.4933 | Nitrogen | 1.8667 | 4.2228 |
| Propylene | 216.5237 | 0.3498 | Oxygen | 1.1169 | 4.4494 |
| 1,3 Butadiene | 222.1383 | 0.3288 | CO2 | 0.3351 | 1.2388 |
| N-butane | 134.4914 | 0.3218 | NH3 | 4.019 | 15.644 |
| Hydrogen | 73.7219 | 0.6273 | VCM | 4.0589 | 15.533 |

The release mass of pipe breakage is calculated by integrating from zero to the leak time t by the release rate equation. The release rate decay factor, λ, is a useful method for approximating the rate of leakage over time. Original model is presented in a study by the Netherlands Organization of applied scientific Research and modified considering on realistic gas flow and decompression characteristics and which acknowledges both the compressibility of the gas and the effects of pipe wall friction in Stephens Research. λ is defined by the ratio of the mass flow at a given point in time and the initial rate of flow and is given by following equation.

$$\lambda = (1 + 0.75t_r)^{-\frac{1}{3}} (20)$$

Since the flow factor, φ, sonic velocity, a_0 and reduced time $t_r$ have different values for each transported fluid, the leakage mass for each material is calculated by reflecting this. The released mass can be calculated from the following integrating equation.

$$\mathrm{M} = \int_0^{t_{release}} [1 + 0.75 \cdot t \cdot a]^{-\frac{1}{3}} dt \text{ (where } a = \frac{f}{2 \cdot d} \cdot \sqrt{\frac{z_u RT}{m}}) (21)$$

f is friction factor, $t_{release}$ is time from pipe damage, $z_u$ is compressibility factor of the gas.

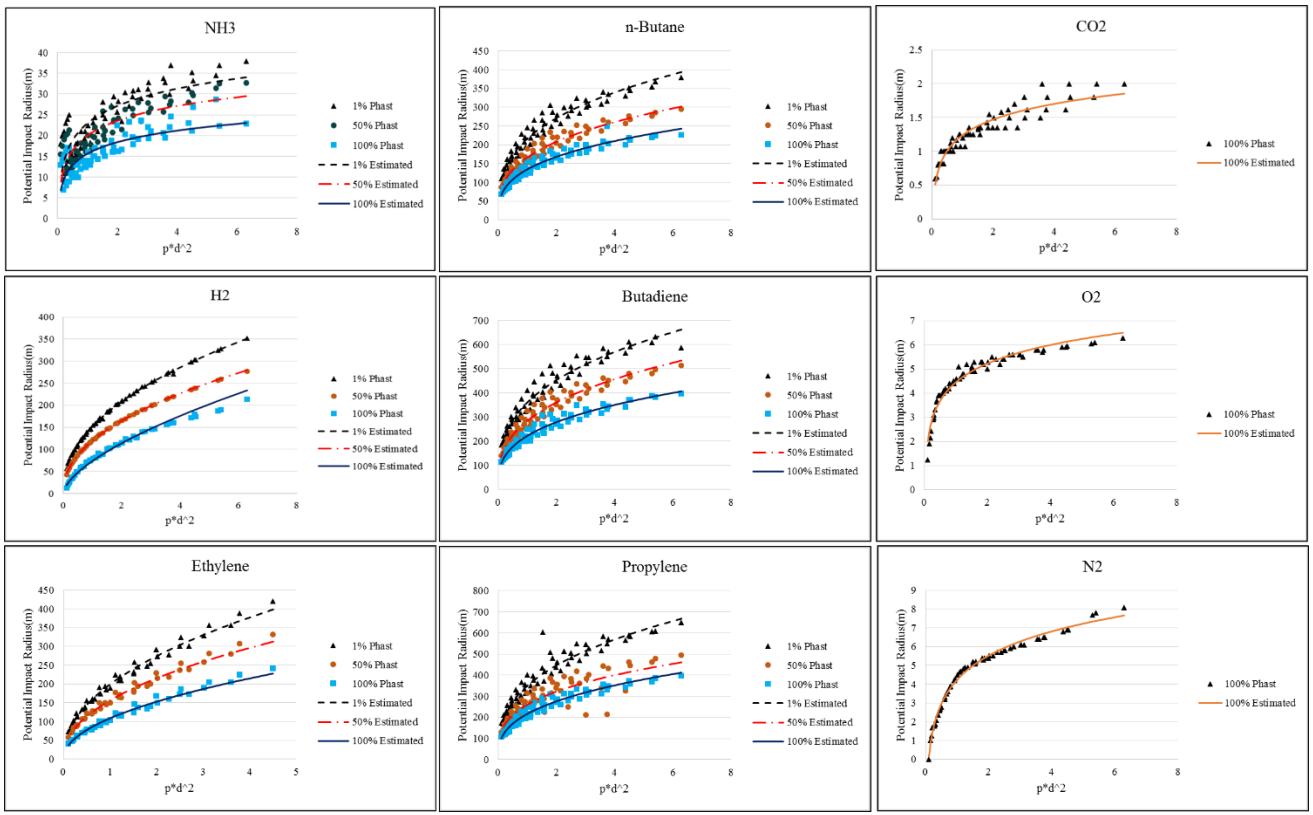


**Figure 3-4 Validation test about Consequence model Result and Phast Simulation Consequence Result**

### 3.3.7. Simulation method

There are various analytical methods in the Structural Reliability Model. First and Second order Reliability Methods ( FORM and SORM) or numerical techniques are possible to calculate the failure probability. Monte-carlo simulation is representative technique because it is independent of the complexity and dimension of the problem. [53]. Meanwhile, Subset simulation (SS) is efficient for estimating small failure probabilities and robust to dimensions. It converts a small failure probability into a product of relatively large conditional probabilities by introducing intermediate events. However, in this study, since the failure frequency and the failure rate are divided into models for the calculation of the failure probability, the MCS is applied without a separate SS configuration. The overall probability calculation for the case study was performed using MATLAB R2018b for MCS. Figure 3-5 shows the MCS results of 6 limit state functions. The failure rate is calculated based on the distribution of the load variable and the resistance variable of each function.

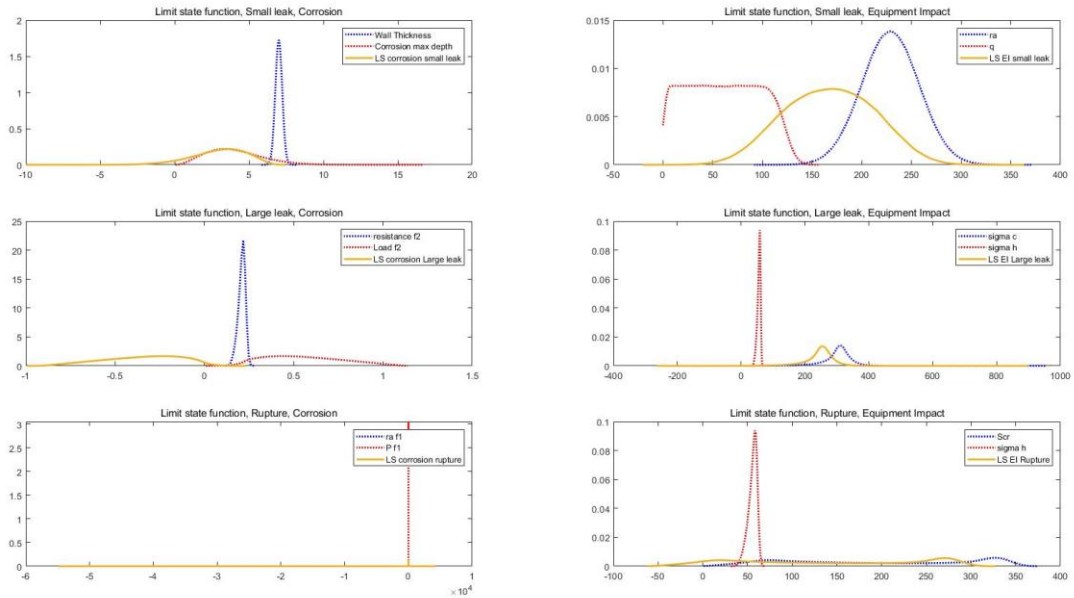


**Figure 3-5. Monte Carlo Simulation Results about 6 Limit State functions**

## 3.4. Case study

In this chapter, a case study is conducted based on the Structural Reliability model of the above-mentioned Underground pipeline. In order to set up the aged piping for this purpose, the pipe which is aged more than 20 years is targeted. The piping information was constructed by reflecting information on actual piping operation status.

### 3.4.1. Statistical review of Industrial complex underground pipeline

The Survey of Ulsan and Yeosu industrial complex was conducted for 84.23% of the length of buried high pressure gas pipelines buried outside the workplace. Each element includes pipe diameter, pressure, year, material, depth of buried, fluid type, patrol period, mode and coating situation. Major fluid types include flammable materials such as Hydrogen, Ethylene, and Propylene, and Toxic materials corresponding to Ammonia. The case conditions were set based on this, and the external corrosion rate of each pipe was estimated to be in accordance with API 581 RP setting value. Factors determining corrosion rate include pipe cover, cathodic protection, soil resistivity, and soil environment. Based on this, a total of eight actual pipe cases were selected. The selection criteria are as follows for more than 20 years. The detailed conditions are in Table 3-8.

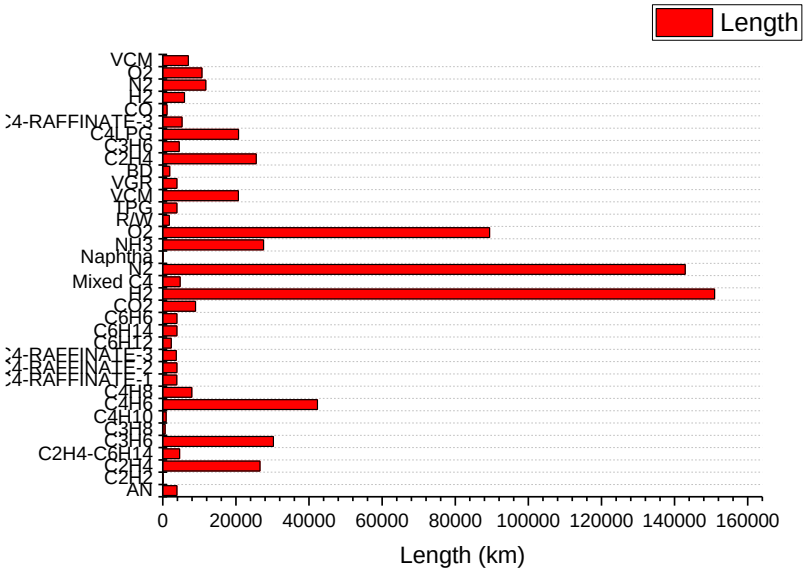


**Figure 3-6 The portion of Ulsan and Yeosu Underground Pipeline working fluids**

**Table 3-7 Test pipeline information**

| Case | Test 1 | Test 2 | Test 3 | Test 4 | Test 5 | Test 6 | Test 7 | Test 8 |
|---|---|---|---|---|---|---|---|---|
| Product | H2 | H2 | NH3 | NH3 | C2H4 | C2H4 | Propylene | Propylene |
| Elapsed Year | 28 | 21 | 34 | 29 | 25 | 22 | 27 | 40 |
| Diameter | 75 | 150 | 250 | 100 | 50 | 150 | 200 | 100 |
| Wall Thickness | 5.49 | 6 | 9.3 | 6.02 | 8.74 | 7.1 | 8 | 6.02 |
| Operating Pressure | 2.9 | 1.8 | 1.9 | 2 | 3.4 | 1.1 | 1.5 | 4.6 |
| Yield Strength | 290 | 290 | 206 | 216 | 290 | 240 | 240 | 240 |
| Tensile Strength | 415 | 415 | 382 | 373 | 415 | 415 | 415 | 415 |
| Length | 4400 | 2100 | 1400 | 5200 | 1200 | 1209 | 3500 | 7200 |
| Linemark | On | On | On | On | On | On | On | On |
| Patrol | 1/quarter | Weekly | Daily Patrol | Daily Patrol | monthly | Weekly | Weekly | Daily Patrol |
| Coating type | Mill Applied PE | Mill Applied PE | Mill Applied PE | Mill Applied PE | Mill Applied PE | Mill Applied PE | Mill Applied PE | Filed Applied PE |
| Cathodic Protection | External CP | External CP | External CP | External CP | External CP | External CP | External CP | External CP |

**Table 3-8. Product property at normal temperature and pressure**

| Product | H2 | NH3 | C2H4 | Propylene |
|---|---|---|---|---|
| Volumetric Cost($/m3) | 0.62916 | 6.255 | 14.136 | 9.05 |
| LFL (vol conc) | 0.04 | 0.15 | 0.027 | 0.02 |
| Heat of combustion(J/kg) | 1.20E+08 | 18646000 | 47195000 | 45799000 |
| Heat of vaporization(J/kg) | 4484126 | 1370000 | 483200 | 435000 |
| Boiling Point(K) | 20.271 | 239.8 | 169.5 | 225.5 |
| Critical Temperature(K) | 33.19 | 406.2 | 283.1 | 365 |

## 3.5. Result and discussion

The results were analyzed for eight test cases. The change of reliability according to the year was observed, and the relative risk comparison and the reliability target were confirmed.

### 3.5.1. Estimation result of failure probability

The 8 cases for H2, NH3, C2H4 and C3H6 were tested for reliability. Compared with the reliability goal, the current pipeline accident probability and future trends can be predicted. As a result of the analysis, it is predicted that the probability of accidents will increase beyond the reliability target within 10 years if the test is 2, 3, 4, 6, 7, 8. Among the cases, the case with the largest absolute value of the accident probability was in the case of the test 1, but it can be judged that it is well managed because it does not exceed the reliability target.

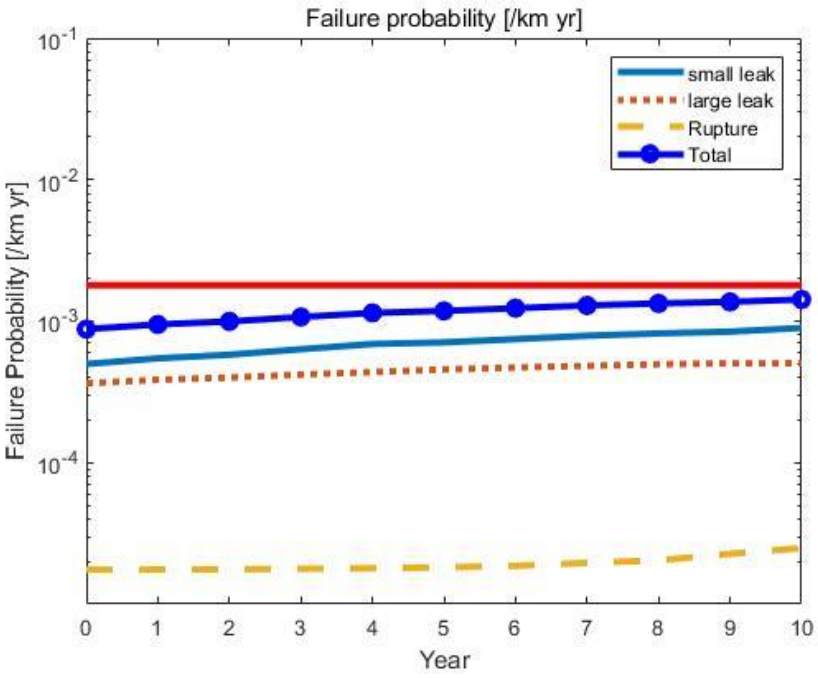


**Figure 3-7 Prediction results of failure probability for Test 1**

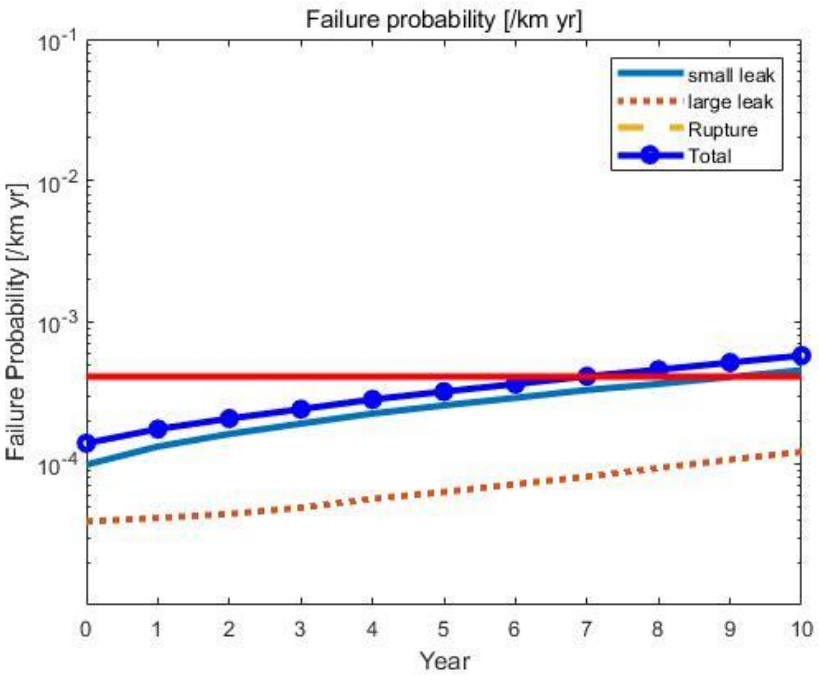


**Figure 3-8 Prediction results of failure probability for Test 2**

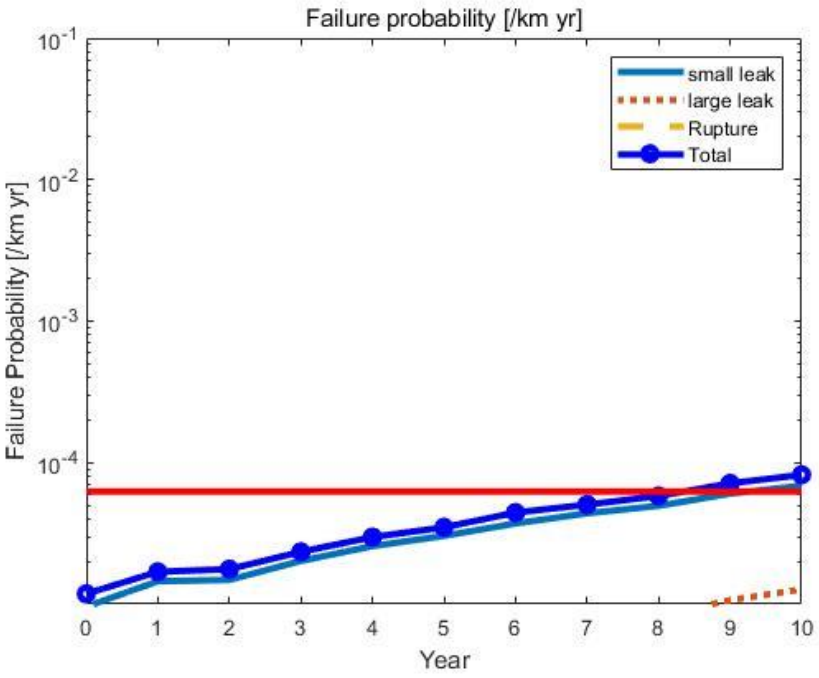


**Figure 3-9 Prediction results of failure probability for Test 3**

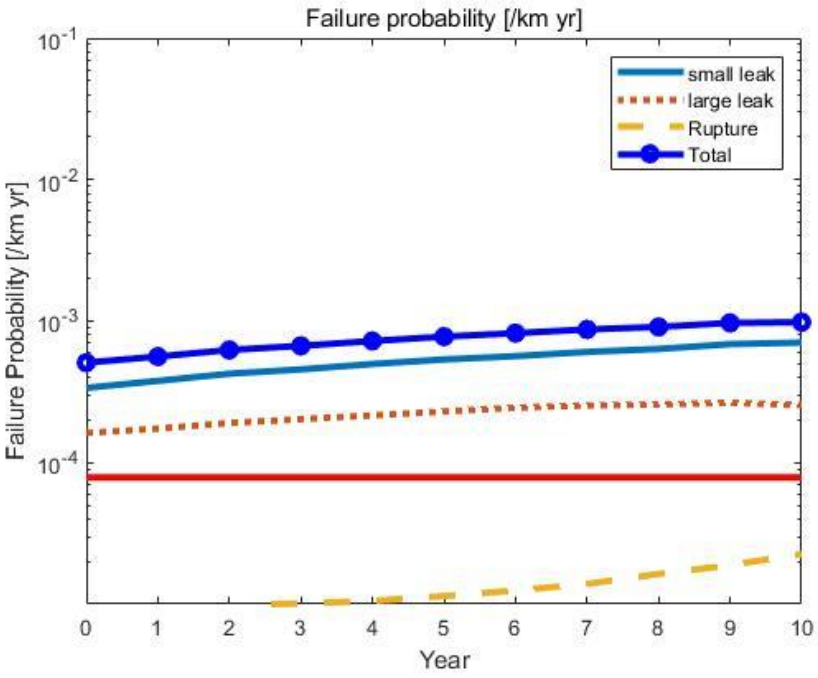


**Figure 3-10 Prediction results of failure probability for Test 4**

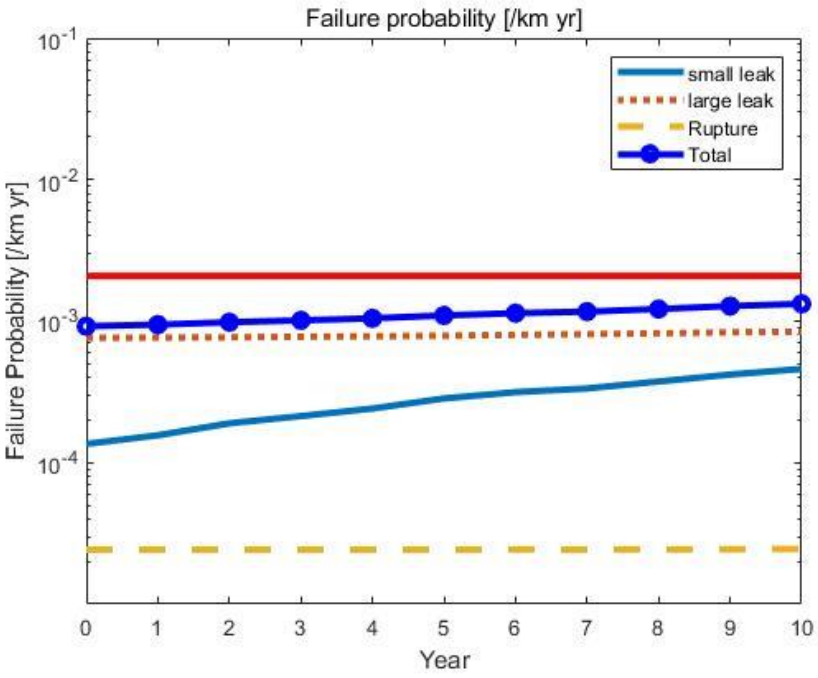


**Figure 3-11 Prediction results of failure probability for Test 5**

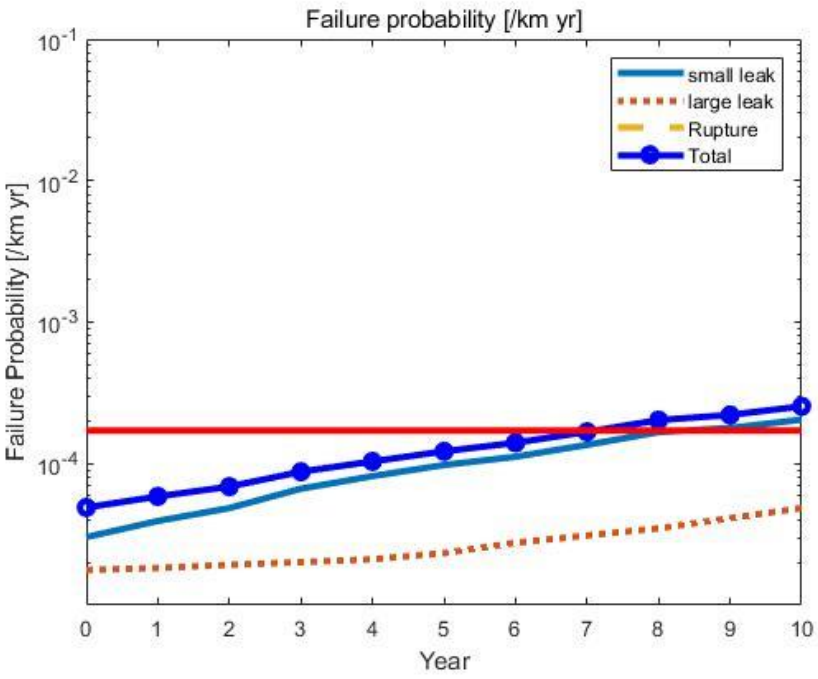


**Figure 3-12 Prediction results of failure probability for Test 6**

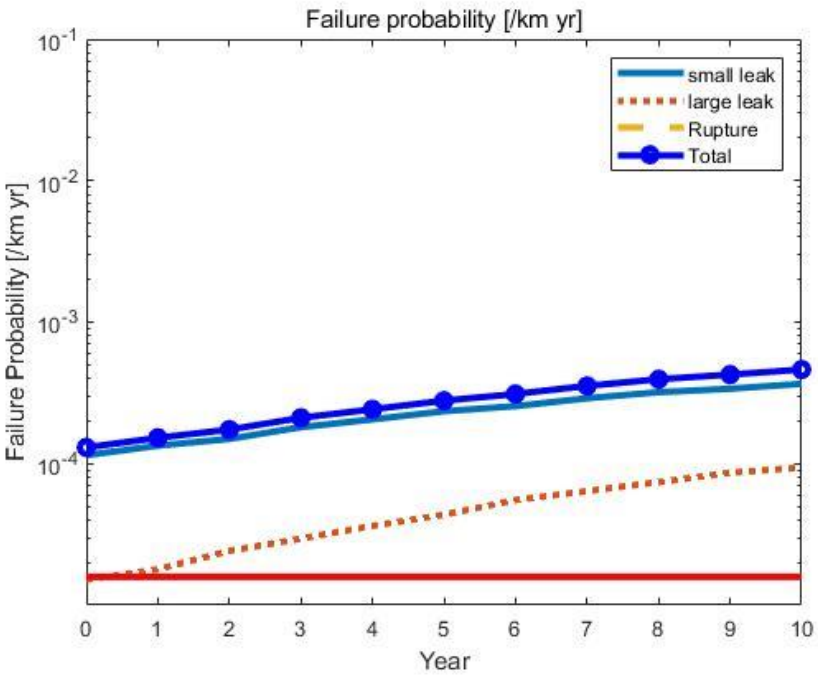


**Figure 3-13 Prediction results of failure probability for Test 7**

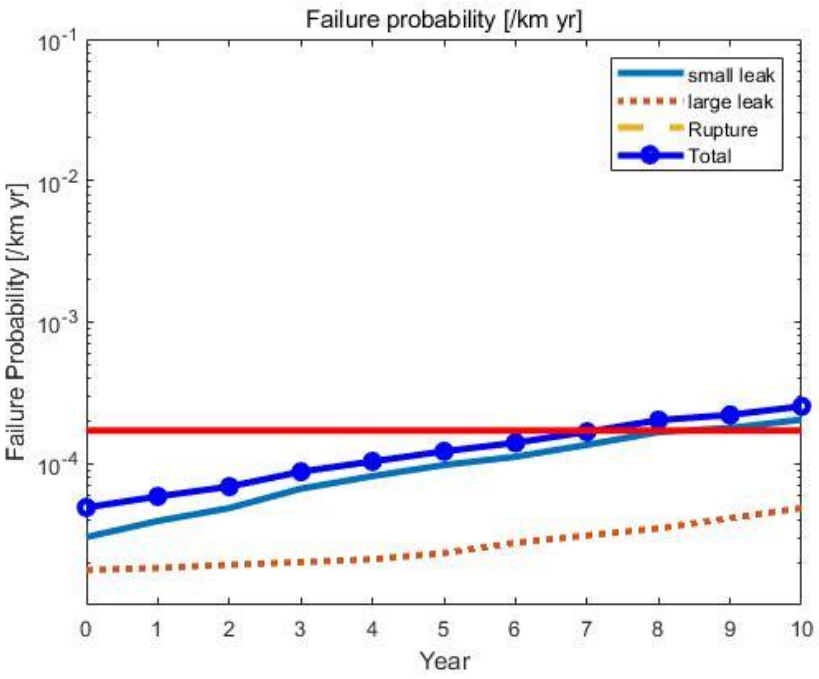


**Figure 3-14 Prediction results of failure probability for Test 8**

**Table 3-9. Failure probability Estimation results (8 Tests)**

| Time(yr) | Test 1 | Test 2 | Test 3 | Test 4 | Test 5 | Test 6 | Test 7 | Test 8 |
|---|---|---|---|---|---|---|---|---|
| 0 | 0.000878 | 0.0001393 | 1.18E-05 | 0.0005088 | 0.0009207 | 4.54E-05 | 0.0001301 | 0.0010704 |
| 1 | 0.0009478 | 0.0001754 | 1.69E-05 | 0.0005616 | 0.0009444 | 5.77E-05 | 0.0001522 | 0.0010975 |
| 2 | 0.000995 | 0.0002082 | 1.77E-05 | 0.0006252 | 0.0009822 | 6.88E-05 | 0.000174 | 0.0011257 |
| 3 | 0.0010693 | 0.0002425 | 2.34E-05 | 0.0006685 | 0.0010126 | 8.18E-05 | 0.0002107 | 0.0011331 |
| 4 | 0.0011428 | 0.000284 | 2.97E-05 | 0.0007235 | 0.0010465 | 0.0001019 | 0.000242 | 0.0011366 |
| 5 | 0.0011809 | 0.0003228 | 3.49E-05 | 0.000777 | 0.0010964 | 0.0001206 | 0.0002786 | 0.0011575 |
| 6 | 0.001234 | 0.0003649 | 4.43E-05 | 0.0008221 | 0.0011383 | 0.0001422 | 0.0003105 | 0.0011555 |
| 7 | 0.0012902 | 0.0004143 | 5.04E-05 | 0.000873 | 0.0011671 | 0.0001657 | 0.0003543 | 0.0011638 |
| 8 | 0.0013341 | 0.0004608 | 5.81E-05 | 0.0009096 | 0.0012178 | 0.0001977 | 0.0003946 | 0.0011552 |
| 9 | 0.0013679 | 0.0005176 | 7.13E-05 | 0.0009712 | 0.0012775 | 0.0002151 | 0.0004258 | 0.0011756 |
| 10 | 0.0014226 | 0.0005802 | 8.20E-05 | 0.0009828 | 0.0013245 | 0.0002566 | 0.000462 | 0.0011981 |
| Reliability Target | 0.0017903 | 0.0004128 | 6.26E-05 | 7.86E-05 | 2.14E-03 | 0.0001529 | 1.59E-05 | 4.38E-05 |

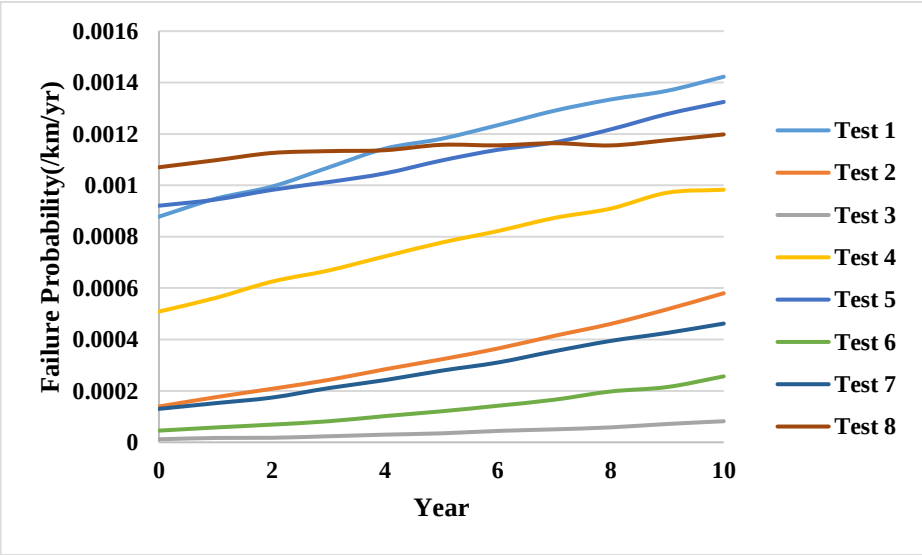


**Figure 3-15 Total failure probability trends of Test cases**

### 3.5.1. Estimation result validation

There is a limit to the verification of the accident probability calculation results. The purpose of this study is to estimate the probability of accident for the purpose of safety management for the chemical equipment accident which is rare in itself, which is trying to calculate the accident probability by using the structural reliability analysis model. The advantage of this method over the existing accident history model is that it is suitable for the management facilities with high uncertainty factors such as underground piping. It can also be useful for the maintenance scenarios analysis that you will proceed in Chapter 4. In the existing accident history model, the effect can be used for the analysis beyond determining whether the specific safety management plan goes beyond the ALARP region.

From the OGP Risk Assessment Data Directory from the UK HSE, the Incident frequency result was compared with the accident occurrence by piping condition. In the reliability analysis process, it is difficult to make exact comparison because factors affecting the corrosion rate or the probability of impact of other construction are affected. Therefore, it was assumed that the condition of general piping is well managed by excluding the extreme situation. In the year of burial, the conditions such as coating type, cathodic protection, soil resistivity, and Soil condition were set as the second best conditions based on the 15 years pipeline.

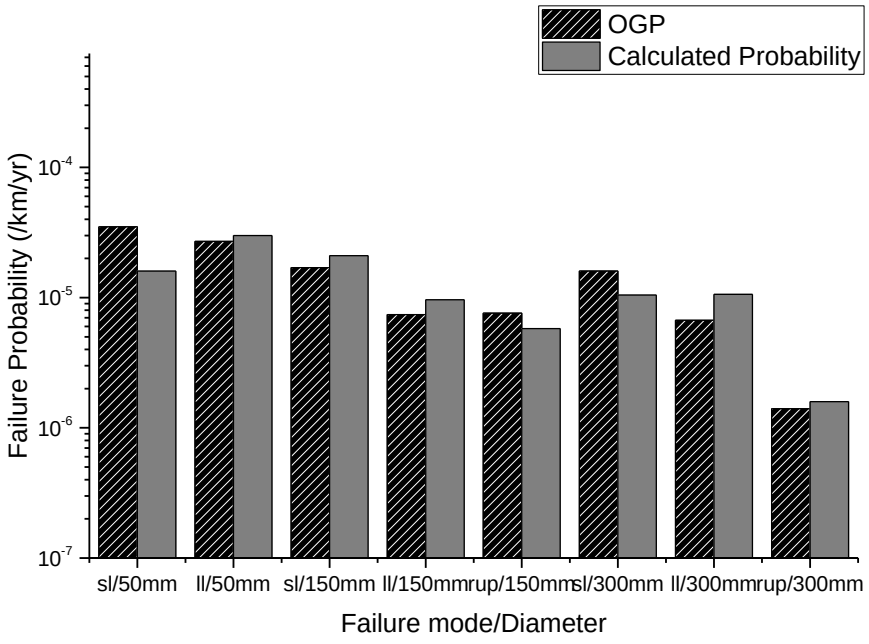


**Figure 3-16 The comparison between OGP Incident frequency data and estimation data**

# CHAPTER 4. Maintenance optimization methodology for cost effective underground pipeline management

## 4.1. Introduction

In order to detect and respond to faults causing major accidents, high-resolution devices such as ILI (Inline-inspection), Hydrostatic Testing, and External Corrosion Direct Assessment (ECDA) can be used.[54, 55] However, for management companies, it is difficult to determine which methodology is cost-effective. In the world, aged pipelines are running in the industrial complex for more than 30-40 years, but there is no precise management system. Appropriate monitoring, inspection, and maintenance of piping can last for longer than the design life, which can be an optimization problem for the management company as there is a tradeoff between the uncertain damage caused by the accident and the costs involved in maintenance and management.

The Cost-Benefit Analysis problem has been a subject of continuous research and various methods have been tried. A framework for diagnosing piping management by using a fuzzy logic model or introducing a risk based inspection concept has been proposed.[56-58]

However, these methodologies are only semi-quantitative and can only be used to prioritize the application of risk measures in piping, and it is difficult to

quantitatively identify actual cost effects. In order to compensate for this, a methodology for evaluating pipeline integrity using a quantitative methodology based on the Structural Reliability Method can be used. [59] Canadian Standards Association(CSA) summarizes the application of reliability based methods to the design and assessment of natural gas transmission pipelines.[60] This method demonstrates the structural adequacy of a pipeline by making an explicit estimate of its reliability and comparing it to a specified reliability target. Structural reliability analysis are obtaining wider acceptance as a basis for evaluating pipeline integrity and these methods are ideally suited to managing metal corrosion damage as identified risk reduction strategies. The essence of this approach is to combine deterministic failure models with maintenance data and the pipeline attributes, experimental corrosion growth rate database, and the uncertainties inherent in this information. The calculated failure probability suggests the basis for informed decisions on which defects to repair, when to repair them and when to re-inspect or replace them.

In recent years, Markov failure model is used in the pipeline failure modeling and maintenance optimization [61, 62]. Provan and Rodrigues are the first authors to use a nonhomogeneous markov process to corrosion defect depth growth. Their model is consists of analytical solutions of the system of Kolmogorov's forward equations. And Several validated markov chain pitting corrosion models are proposed in the past researches.

The statistical model for pitting corrosion is known to be the Gumbel and Weibull distributions using the Maximum Likelihood Estimator.[11] This can be used to estimate the life span, or reliability analysis can be performed by calculating the specific pipe accident probability. Finally, optimization of piping management costs is possible. Kong Fah Tee conducted the reliability-based life-cycle cost optimization using the genetic algorithm by dividing the failure mode of the pipe into deflection, buckling, and wall thrust.[14] This algorithm can help find the optimal maintenance action at maintenance total cost. However, this study did not consider the rigorous consequence model that affects the expected failure cost. In addition, there are limitations in that it is impossible to analyze various scenarios in managing one pipeline. M. Al-Amin has conducted reliability assessments on corrosion piping based on inspection data, but has limitations in predicting maintenance actions.

In this paper, we propose pipeline maintenance optimization framework by integrating probabilistic model and reliability evaluation method to predict existing pipe accident probability. Finally, this study demonstrates a case study on the aged industrial complex in Korea using the constructed framework and prove the effectiveness of this methodology. In order to predict the accident probability, failure mode and limit state function are defined and Markov chain Montecarlo simulation is used. In addition, a hit frequency model for defect density modeling and other construction accident probability prediction is

established. The pipeline incident model consists of a linear defect density growth model and a fault tree analysis model, which uses coating damage survey data and equipment impact frequency data from the pipe management company and Korea Gas Safety corporation.

In order to make optimization framework accurately, proposed method involve the Potential Impact Radius and the Spill volume model to overcome the limitations of previous studies that uniformly applied the failure cost. Based on this, the consequences in the three failure modes are predicted and quantified as cost. Figure 1 shows the summarized proposed methods. Using this framework, Pipeline Maintenance Optimization is performed in two steps. First step, maintenance priority diagnosis analysis is performed on the target pipe group. In the second stage, Maintenance Optimization analysis is performed on the most priority managed piping. In this process, we use a diagnostic cycle that meets the reliability criteria and a diagnostic method to find a methodology that minimizes the total cost. Through these two stages of framework, maintenance optimization is possible using structural reliability analysis. The proposed framework can help pipeline safety decision maker to decide when and how to mitigate the pipeline threat factors, which could be reduce the corrosion failure and equipment impact at the minimum cost.

## 4.2. Problem Definition

In order to reduce risk of the pipeline degradation, it is possible to apply various maintenance operations, such as regular inspection to detect the defect, repair action to recover existing damage, replacement of pipeline and preventive actions for accident equipment impact. The optimal maintenance planning should be considered safety point of view and cost-benefit point of view. [63]. Inspection time and re-inspection interval is a fundamental problem for maintenance quality and safe operation of underground pipelines. Failure consequence assessment and probabilistic modelling of inspection results on the basis of SRA allows us to establish and to optimize the maintenance strategies of aging pipeline by satisfying reliability target and availability economic requirements.

Previous chapter describes the SRA model of underground pipeline from failure probability calculation to consequence assessment. This chapter formulate the additional maintenance model such as expected cost model and mitigation effect model. Finally several scenario comparison studies are performed to find optimal maintenance action through minimize the expected total cost satisfying several requirements.

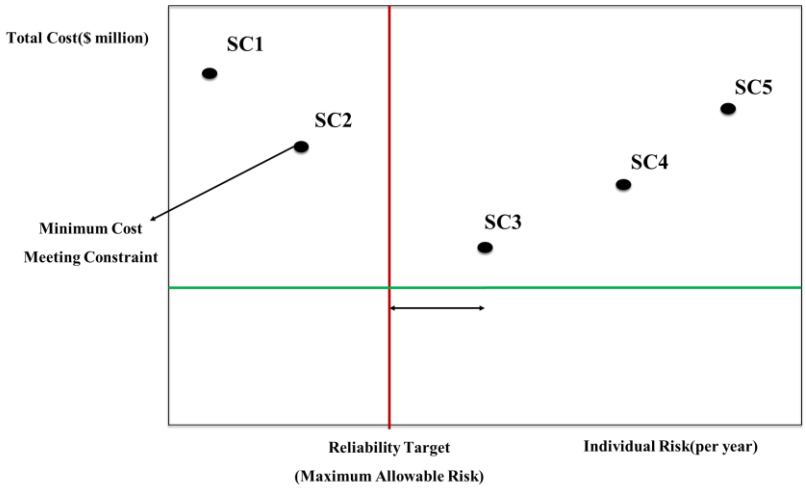


**Table 4-1 Conceptual diagram for underground pipeline maintenance optimization.**

## 4.3. Maintenance scenario analysis modeling

The goal of maintenance optimization is to determine the re-inspection period or specific method under various underground pipeline conditions. Defect repair, direct inspection and indirect inspection are representative integrity methods.

Indirect test methods are hydrostatic test, high resolution ILI, low resolution ILI, and ECDA. ILI is a methodology for measuring the depth and length of a defect by scanning the surface of a pipe through a Pig device using a magnetic field. ECDA is a process to selectively identify high-risk piping in the pre-Direct Assessment stage, and DCVG and CIPS are representative. Hydrostatic test is a method to verify the safety of piping by confirming the rupture and leakage when pressurized with test pressure. Since each methodology has different detection power and accuracy, the effects are also different. The probability of detection model and the Rehabilitation Logic were implemented as a mathematical model for the quantification of this effect.

Finally, we can find the scenario conditions that satisfy the reliability and various marginal conditions with total cost as the main objective function. Through this, it is possible to grasp the best management method for the piping with the high risk rank identified by the structural reliability analysis.

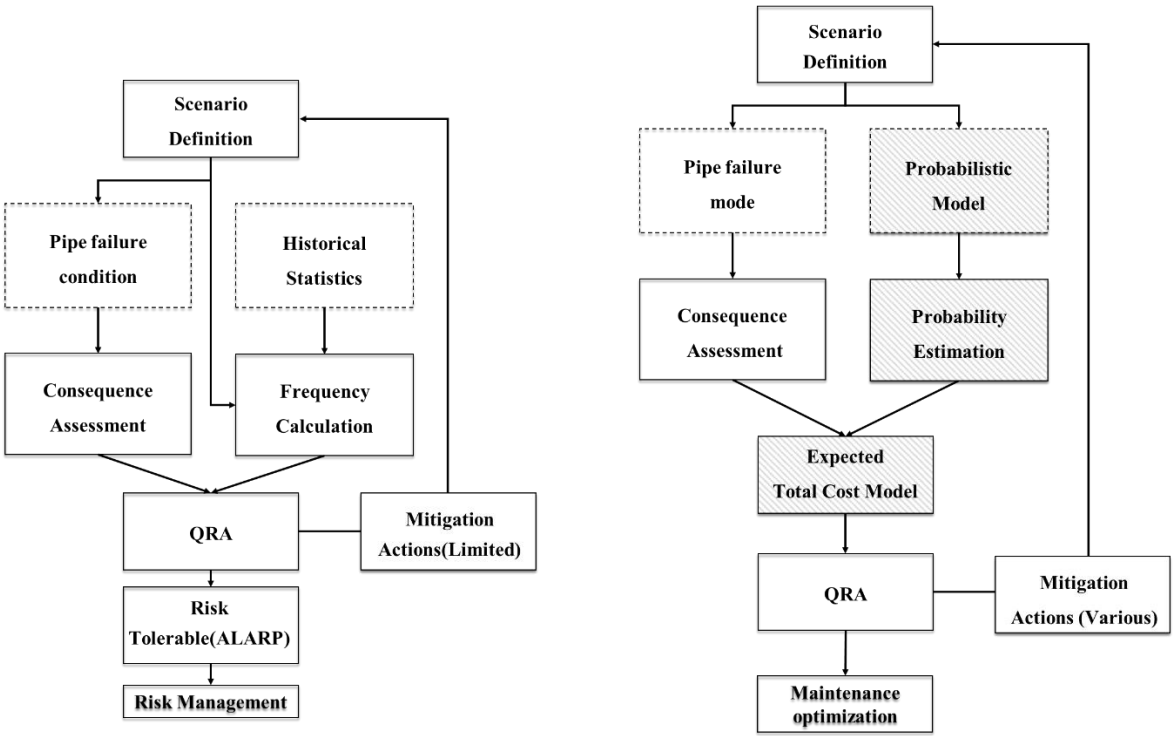


**Figure 4-1 Methodology Comparison between conventional QRA and proposed QRA based on SRA (Left)General QRA, (Right)SRA based QRA**

### 4.3.1. Methodology description

Conventional QRA follows system definition, hazard identification, Consequence Assessment(CA), Frequency Assessment(FA) and risk assessment in order. Using QRA, Pipeline safety can be managed in tolerable region, as low as reasonably practicable(ALARP). The standard of ALARP follows criteria of HSE(Health and Safety Executive). [64]. In this method, it can treat operation condition and pipeline replacement before life time as mitigation options. This is due to the limitation that the result of the inspection or maintenance is not adaptable because the frequency analysis is calculated by historical based model. In real pipeline maintenance problem, it should be considered regular patrol period and inspection.

However, SRA based QRA provides a probabilistic approach to corrosion defect management that addresses the key sources of uncertainty and discriminates between failure modes. This approach can be used to analyze corrosion integrity based on in-line inspection or coating damage survey data, schedule defect repairs and provide guidance in establishing re-inspection intervals. Maintenance optimization can be performed through a total cost value that combines calculated accident probability and consequences for various possible scenarios for piping management. Depending on the type of inspections and the timing of inspection, the defect location and size information are different, and the risk reduction effect is also changed

accordingly. Based on SRA-based QRA, current scenarios can provide a solution for what is a better pipeline integrity methodology under target reliability and reasonable cost marginal conditions.

### 4.3.2. Cost modeling

In order to compare various integrity scenario, specific quantities are defined as a basis for comparison. The cost related to pipeline failure risk and maintenance provide way to determine how to mitigate the pipeline management failure cost-effectively. The cost benefit analysis(CBA)be used as an pipeline maintenance optimization problem. CBA is used to determine the net benefits to the status quo[20]. The quantification of failure risk and maintenance should be same monetary unit. This study use the total cost and net benefit-necessary cost ratio as follows.

$$C_{total}(t) = C_{main}(t) + C_{exf}(\mathrm{t}) (22)$$

$$C_{main}(t) = C_{ma} \cdot Len_i + \sum_{i}^{3} F_{cp}(t) \cdot Len_i \cdot C_i(t) \ (23)$$

$$F_{cp}(t) = \frac{r}{[1-(1+r)^{-t}]} (24)$$

$$C_i(t) = C_{ini} + C_i \cdot N_i(t) (25)($$

$$C_{exf}(t) = C_{pro} + a_n \cdot n_j \cdot f_j(t) (26)$$

Total cost is the sum of the direct costs associated with pipeline inspection and maintenance and the risk related costs associated with pipeline failure including the value of compensation for property damage and human casualties. $C_{main}$ is the cost related to pipeline inspection, excavation, repair, $C_{ma}$ is the annual component of the maintenance cost, $F_{cp}$ is capital recovery factor, $Len_i$ is the length of effective pipeline integrity action, $C_i(t)$ is cost of a defect excavation and repair and inspection, $N_i(t)$ is calculated number of defect excavations or repairs for pipeline. $C_{exf}$ is the expected failure cost, $a_n$ has meaning about economic value of loss of life. Fatality compensation payments for loss of life are based primarily on estimates of the economic value of a human life. In the United Kingdom, the Value of Prevention fatality (VPF) is used for cost benefit analysis of safety measures. This is a value used in the cost benefit analysis as another way of expressing how much you can pay to reduce the average risk of a person. The smallest VPF value is used so that Benefit analysis is not excessively set in the values used in developed countries.

**Table 4-2 Value of preventing fatalities**

| Classification | VPF (Value of preventing fatalities) | VPF Conversion value(₩) | Reference |
|---|---|---|---|
| DOT(2016), USA, $ | 5,800,000 | 6,570,000,000 | [65] |
| Health and Safety Executive(HSE), 2003, UK, £ | 1,336,800 | 1,940,000,000 | [66, 67] |
| C-FER Technologies, Canada, $ | 915,000 | 1,030,000,000 | [68] |

### 4.3.3. Maintenance mitigation model

The purpose of this model is to quantify the maintenance effect. The basic assumptions for this are as follows.

(a) Defects of piping naturally increase gradually as time goes by, which does not disappear by itself.

(b) Defect size and growth rate are different, Defect depth is Weibull distribution, and Defect length is log-normal distribution.

(c) Defects in piping can be detected through the Integrity method, and the accuracy and scope of the detection will vary from method to method.

(d) Defects which are judged to exceed the threshold of the critical stress of the pipe are removed.

(e) There is an excavation and repair criterion for the prediction of future inspection and maintenance activities.

(f) The defect density of the pipe is changed through the defects created and the defects removed by the integrity action.

It is the defect detection accuracy of each methodology that can quantify and distinguish the various test methods. This is confirmed by the following detection probability equation.

$$\text{Probability of Detection(POD)} = 1 - e^{(-q \times d_{avg})}$$

q is constant characterizing tool accuracy, $d_{avg}$is defect depth. Probability of detection modeled as an exponential function. q-value is from the vendor information. However, in this thesis, a fixed q-values at specific inspection method are used. This information is referenced by “specifications and requirements for intelligent pig inspection of pipelines” on pipeline operator forum.

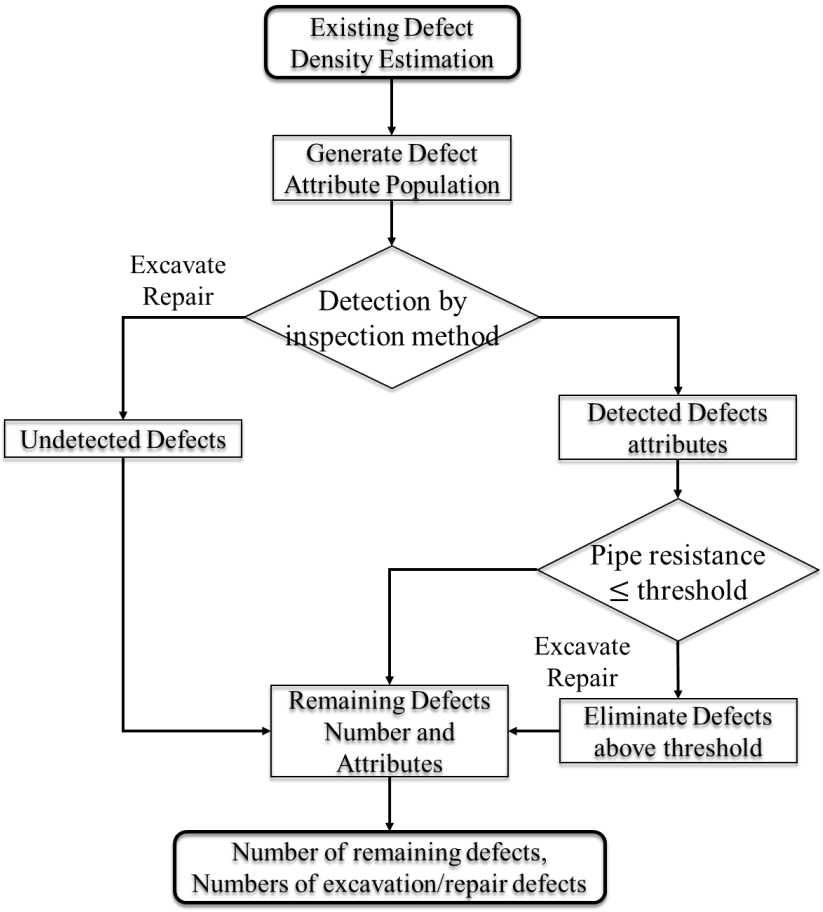


**Figure 4-2 Rehabilitation Logic about underground pipeline**

**Table 4-3. Rehabilitation model for each inspection type**

| Inspection Type | Detectable | Excavation & Rehabilitation Threshold |
|---|---|---|
| Hydro-testing | $P_d = 1 \quad for\ r_a \le P_t$<br>$(P_t : test\ pressure,$<br>$r_a : actual\ pressure\ resistance)$<br>$P_d = 0 \quad for\ r_a \le P_t$ | All should be excavated.<br>Replacement(Detection) |
| Inline Inspection(Pigging) | $P_d = 1 - e^{-q/A}$<br>$A = \frac{\pi}{4} h \cdot l$<br>$(\text{h: maximum depth, l : defect length})$<br>$q = -\ln[1 - P_d(A_r)]/A_r$ | $g_e \le g_e^*$<br>$= 1.6(ILI\ Excavation\ Criterion),\ high\ ILI$<br>$g_e = 100 \times \frac{t_n - h_{max}}{t_n}, g_e \le 20,\ Low\ ILI$<br>$g_r \le g_r^*$<br>$(ILI\ Repair\ Criterion),\ High,\ Low\ ILI$ |
| DCVG, CIPS(Indirect inspection) | $P_d = 0.7$ | $g_e = 100 \times u, \le g_e^*$<br>coating damage threshold, |

## 4.4. Case study

Scenario analysis was conducted on the test cases that were the most dangerous among the test cases set in Chapter 3. In the scenario analysis, it is possible to check how the cost result varies depending on the inspection method selection and the re-inspection cycle. Finally, the optimum value is determined by setting the reliability target and the repair cost limit. When the forecast period is set to 20 years through this study, the total cost of each scenario over the next 10 years will be compared and the annual probability change will be estimated. 10 scenarios were set up for the case study as follows. Inspection method, Inspection Period, and time of next inspection were used as variables.

**Table 4-4. Scenario Comparison study for maintenance optimization**

| Scenario | Method | Inspection Period | Next inspection yr |
|---|---|---|---|
| Scenario 1 | ECDA | 3 | 2 |
| Scenario 2 | ILI(High) | 3 | 2 |
| Scenario 3 | ECDA | 4 | 3 |
| Scenario 4 | ILI(High) | 4 | 3 |
| Scenario 5 | ECDA | 5 | 2 |
| Scenario 6 | ILI(High) | 5 | 2 |
| Scenario 7 | ILI(Low) | 4 | 3 |
| Scenario 8 | Hydrotest | 4 | 3 |
| Scenario 9 | ECDA | 4 | 2 |
| Scenario 10 | Hydrotest | 4 | 2 |

## 4.5. Results

Among the test conditions conducted in Chapter 3, we have analyzed the scenario for the pipeline that meets the reliability target level but is expected to exceed the reliability target within the next 10 years. Based on this, we calculate the maximum probability of accident, the total integrity and the risk cost within the analysis period under the scenario conditions, and find the optimum piping management scenario.

### 4.5.1. Result of optimal re-inspection period

In the test case, Scenario1, 5, and 9 are all the same and only the analysis period is different. Then, it can be confirmed that the 4-year cycle analysis is ideal because the management cost can be minimized when the reliability is not exceeded.

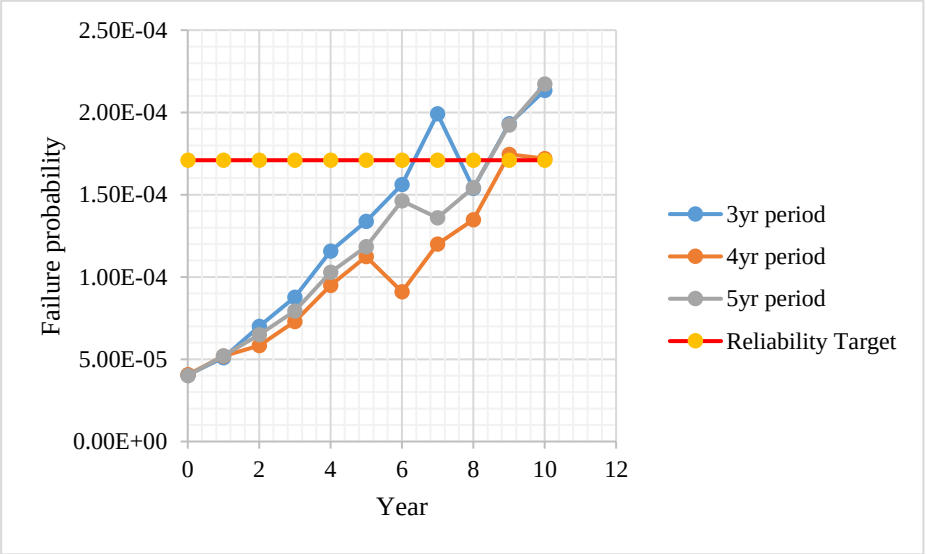


**Figure 4-3. Optimal re-inspection analysis about ethylene underground pipeline(Failure probability)**

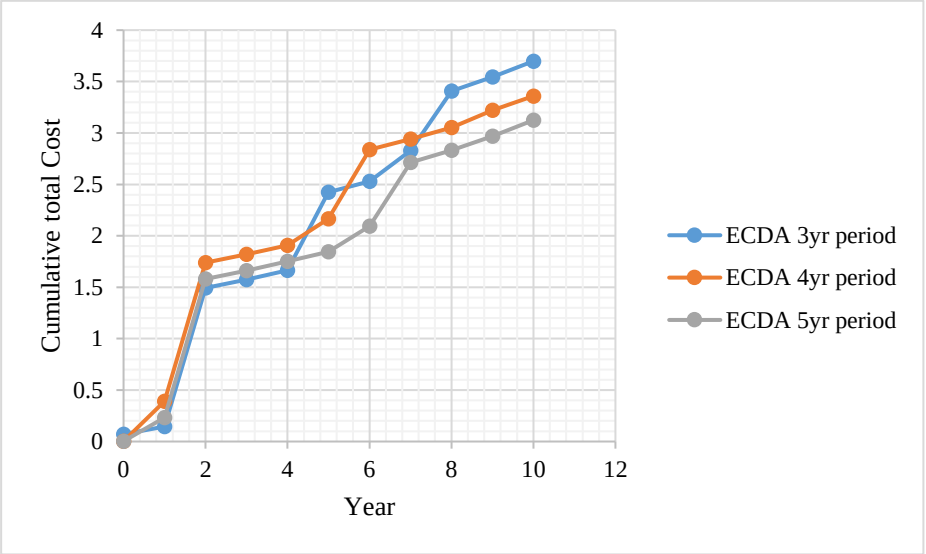


**Figure 4-4. Optimal re-inspection analysis about ethylene underground pipeline(Cumulative Total cost)**

**Table 4-5. Scenario comparison study for finding maintenance optimal actions**

| Sum of total cost | 3.698533266 | 4.867149228 | 3.014355892 | 3.290583433 | 3.19316556 | 4.095957751 | 1.854357094 | 5.930043158 | 3.429048829 | 5.710687634 |
|---|---|---|---|---|---|---|---|---|---|---|
| Max Failure probability | 2.13E-04 | 1.07E-04 | 7.66E-05 | 8.66E-05 | 2.17E-04 | 1.09E-04 | 2.15E-04 | 6.99E-05 | 1.75E-04 | 5.19E-05 |
| RT | 0.00017095 | 0.00017095 | 0.00017095 | 0.00017095 | 0.00017095 | 0.00017095 | 0.00017095 | 0.00017095 | 0.00017095 | 0.00017095 |
| Total Cost | ECDA | ILI(High) | ECDA | ILI(High) | ECDA | ILI(High) | ILI(Low) | Hydrotest | ECDA | Hydrotest |
| Year | Scenario 1 | Scenario 2 | Scenario 3 | Scenario 4 | Scenario 5 | Scenario 6 | Scenario 7 | Scenario 8 | Scenario 9 | Scenario 10 |
| 0 | 0.071107549 | 0.004079423 | 0.071464464 | 0.00385799 | 0.07146042 | 0.003854362 | 0.003968743 | 0.06146042 | 0.072646472 | 0.003146042 |
| 1 | 0.073467861 | 1.260705745 | 0.073427049 | 0.005820575 | 0.230084064 | 1.416744016 | 0.005838279 | 1.573670791 | 0.387903515 | 1.573499543 |
| 2 | 1.349326945 | 1.805620174 | 0.501843895 | 1.070592075 | 1.348913966 | 1.804724573 | 0.328067497 | 1.176540369 | 1.348965699 | 2.468705827 |
| 3 | 0.080445962 | 0.00365941 | 1.044633548 | 1.373256461 | 0.080649802 | 0.002608749 | 0.757712353 | 1.797268804 | 0.080291132 | 0.081999352 |
| 4 | 0.089890711 | 0.007620862 | 0.08271501 | 0.003777134 | 0.087841052 | 0.005518635 | 0.015836738 | 0.067266009 | 0.087047309 | 0.134688208 |
| 5 | 0.760084345 | 0.950948991 | 0.088096117 | 0.005122411 | 0.094628036 | 0.00736963 | 0.022954617 | 0.057929763 | 0.259961138 | 0.115789181 |
| 6 | 0.106967011 | 0.013312962 | 0.142708622 | 0.00673756 | 0.249681287 | 0.010259867 | 0.078395241 | 0.051512277 | 0.669827112 | 1.07228276 |
| 7 | 0.295957264 | 0.065037483 | 0.615533539 | 0.739684107 | 0.618977909 | 0.743651517 | 0.435381952 | 0.998807206 | 0.103823305 | 0.047131082 |
| 8 | 0.579217063 | 0.677158027 | 0.113751809 | 0.017304501 | 0.118528483 | 0.022632189 | 0.050864361 | 0.044181753 | 0.112979915 | 0.044068899 |
| 9 | 0.139793434 | 0.036382654 | 0.132283085 | 0.028745161 | 0.13804743 | 0.035220686 | 0.070699572 | 0.084478218 | 0.168642254 | 0.084738997 |
| 10 | 0.152275122 | 0.042623498 | 0.147898754 | 0.035685458 | 0.154353109 | 0.043373526 | 0.084637742 | 0.016927548 | 0.136960978 | 0.084637742 |

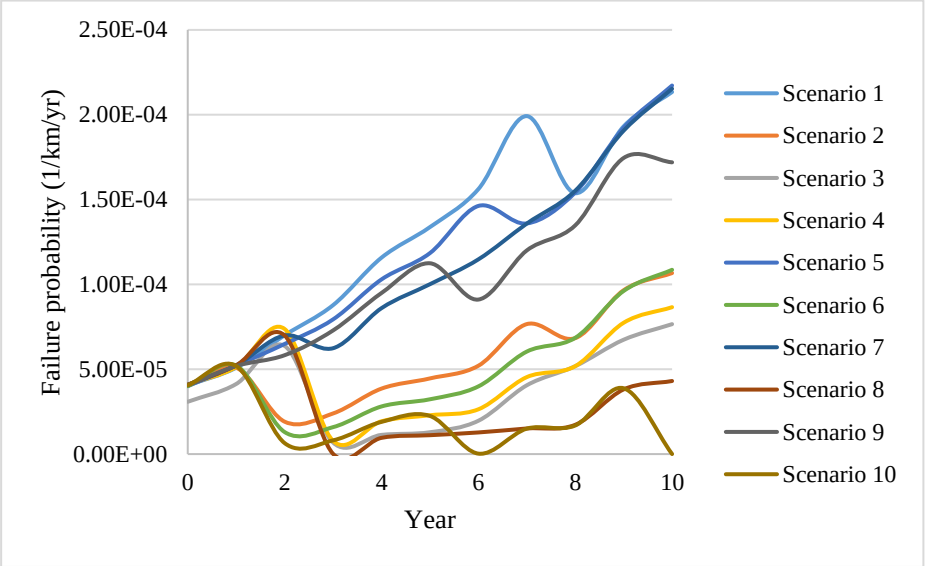


**Figure 4-5. Scenario comparison result of failure probability trend**

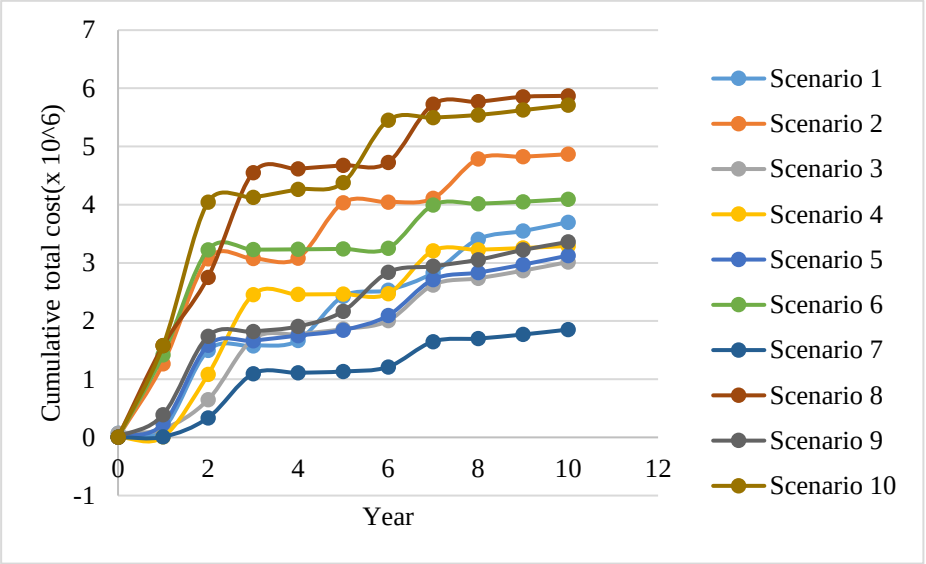


**Figure 4-6. Scenario comparison result of cumulative total cost**

### 4.5.2. Result of optimal maintenance actions

Among the 10 scenarios, there are two scenarios that satisfy the reliability target and the maintenance budget. In particular, it can be seen that Scenario 3 in the left-down direction is more appropriate.

This analytical methodology is not an optimization in the strict sense but it is confirmed that it can help to find the optimal strategy by comparing the conservative scenarios with the constraint of cost and reliability.

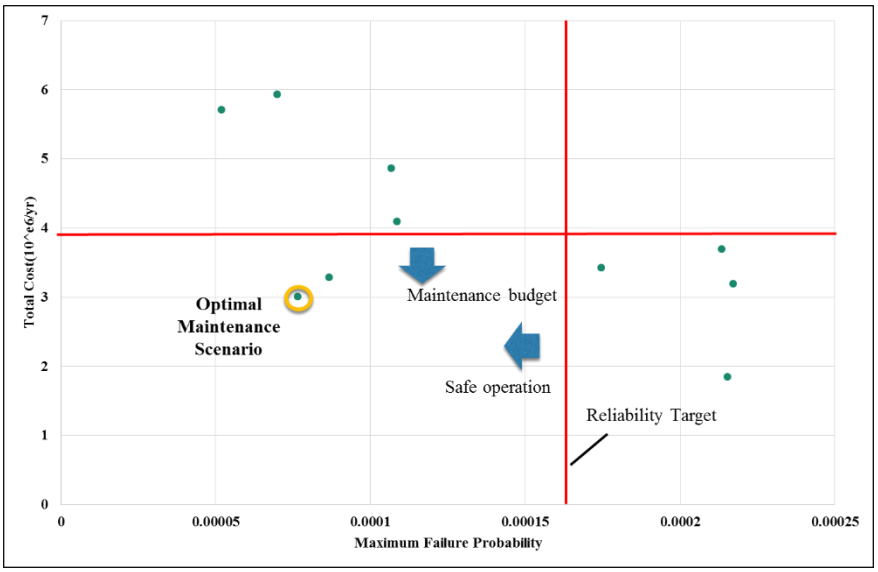


**Figure 4-7. optimal maintenance scenario considering maintenance budget and safety simultaneously**

# CHAPTER 5. Concluding Remarks

This thesis has addressed the Life time Estimation for two industrial system considering system uncertainty.

First problem is related to state of health in battery management system. State of health is life time indicator to diagnose life cycle phase about battery. Using observer technique or least square parameter estimation approach, SOH can be estimated through value of capacity fade. In this study, SOH algorithm which can be easily applied to various ESS sites was developed and verified. It predicts SOH through Capacity fade estimation based on SOC and RLS using EKF technique. SOH estimation method is verified based on the 1 cell test and 2 application sites.

Second problem is about aged underground pipeline management. Appropriate inspections and maintenance repairs are essential for safe maintenance of aged piping over its design life. However, there are not many methodologies to quantify the cost of safety management, and there is a strong tendency to rely on experienced safety experts. Chapter 3 introduced the structural reliability analysis and conducted basic modeling to solve the underground piping management optimization problem. In the generalized quantitative risk assessment, the FA part was replaced with the probabilistic

model and the limit state function to reflect the effect of the undetermined elements of the buried underground piping. In Chapter 4, we conducted maintenance optimization modeling to adopt optimal inspection cycle and inspection methodology. To do this, we introduced a cost model consisting of Expected failure cost and maintenance cost and a quantitative model to reflect the risk reduction effect on each methodology. Finally, based on the 10 scenarios, the optimal scenario was selected when the reliability target and the cost were limited. Based on this study, we quantitatively modeled the indeterminate elements of the system and solved the consequences of it statistically. In Chapter 2, we confirmed that it is a SOH prediction algorithm with better accuracy, and through Chapter 3, 4, we can select the optimal strategy among the maintenance scenarios.

# References


1. Marc C. Kennedy, A.O.H., *Bayesian calibration of computer models.* Journal of the Royal statistical society, 2001. **Series B Volume 63**: p. pp425-464.
2. Ronald L. Iman, J.C.H., *An Investigation of Uncertainty and sensitivity analysis Techniques for Computer Models.* Risk Analysis, 1988. **Volume 8**(Issue 1): p. 71-90.
3. W.E. Walker, P.H., J. Rotmans, J.P. van der Sluijs, M.B.A. van Asselt, P. Janssen and M.P. Krayer von Krauss, *Defining Uncertainty : A Conceptual Basis for Uncertainty Management in Model based Decision Support.* Integrated Assessment, 2003. **4**(1).
4. Jingshan Li, S.Z., Yehui Han, *Advances in Battery Manufacturing, Service, and Management Systems*. 2016: IEEE Press.
5. DeWolf, G.B., *Process safety management in the pipeline industry: parallels and differences between the pipeline integrity management (IMP) rule of the Office of Pipeline Safety and the PSM/RMP approach for process facilities.* Journal of Hazardous Materials, 2003. **104**(1-3): p. 169-192.
6. Dunn, B., H. Kamath, and J.-M. Tarascon, *Electrical Energy Storage for the Grid: A Battery of Choices.* Science, 2011. **334**(6058): p. 928.
7. M.M. Thackeray, C.W., and E.D. Isaacs, *Electrical energy storage for transportation approaching the limits of, and going beyond, lithium-ion batteries.* Energy Environment Science, 2012. **5**: p. 7854-7863.
8. Bhangu, B.S., et al., *Nonlinear observers for predicting state-of-charge and state-of-health of lead-acid batteries for hybrid-electric vehicles.* IEEE Transactions on Vehicular Technology, 2005. **54**(3): p. 783-794.
9. Ng, K.S., et al., *Enhanced coulomb counting method for estimating state-of-charge and state-of-health of lithium-ion batteries.* Applied Energy, 2009. **86**(9): p. 1506-1511.
10. Kim, I., *A Technique for Estimating the State of Health of Lithium Batteries Through a Dual-Sliding-Mode Observer.* IEEE Transactions on Power Electronics, 2010. **25**(4): p. 1013-1022.
11. Xing, Y., et al., *Battery Management Systems in Electric and Hybrid Vehicles.* 2011. **4**(11): p. 1840.
12. Garche, J., A. Jossen, and H. Döring, *The influence of different operating conditions, especially over-discharge, on the*

*lifetime and performance of lead/acid batteries for photovoltaic systems.* Journal of Power Sources, 1997. **67**(1): p. 201-212.

13. Zou, Y., et al., *Combined State of Charge and State of Health estimation over lithium-ion battery cell cycle lifespan for electric vehicles.* Journal of Power Sources, 2015. **273**: p. 793-803.

14. Weigert, T., Q. Tian, and K. Lian, *State-of-charge prediction of batteries and battery–supercapacitor hybrids using artificial neural networks.* Journal of Power Sources, 2011. **196**(8): p. 4061-4066.

15. Salkind, A.J., et al., *Determination of state-of-charge and state-of-health of batteries by fuzzy logic methodology.* Journal of Power Sources, 1999. **80**(1): p. 293-300.

16. Singh, P., et al., *Design and implementation of a fuzzy logic-based state-of-charge meter for Li-ion batteries used in portable defibrillators.* Journal of Power Sources, 2006. **162**(2): p. 829-836.

17. Singh, P., C. Fennie, and D. Reisner, *Fuzzy logic modelling of state-of-charge and available capacity of nickel/metal hydride batteries.* Journal of Power Sources, 2004. **136**(2): p. 322-333.

18. Plett, G.L., *Extended Kalman filtering for battery management systems of LiPB-based HEV battery packs: Part 3. State and parameter estimation.* Journal of Power Sources, 2004. **134**(2): p. 277-292.

19. Plett, G.L., *Sigma-point Kalman filtering for battery management systems of LiPB-based HEV battery packs: Part 1: Introduction and state estimation.* Journal of Power Sources, 2006. **161**(2): p. 1356-1368.

20. Hansen, T. and C.-J. Wang, *Support vector based battery state of charge estimator.* Journal of Power Sources, 2005. **141**(2): p. 351-358.

21. Kim, J., S. Lee, and B.H. Cho, *Discrimination of Li-ion batteries based on Hamming network using discharging–charging voltage pattern recognition for improved state-of-charge estimation.* Journal of Power Sources, 2011. **196**(4): p. 2227-2240.

22. Lee, S., et al., *State-of-charge and capacity estimation of lithium-ion battery using a new open-circuit voltage versus state-of-charge.* Journal of Power Sources, 2008. **185**(2): p. 1367-1373.

23. Wang, J., et al., *Combined state of charge estimator for electric vehicle battery pack.* Control Engineering Practice, 2007. **15**(12): p. 1569-1576.

24. Ossai, C. and N. Raghavan, *Statistical Characterization of the State-of-Health of Lithium-Ion Batteries with Weibull Distribution Function—A Consideration of Random Effect Model in Charge Capacity Decay Estimation.* 2017. **3**(4): p. 32.

25. Liu, D., et al., *Prognostics for state of health estimation of lithium-ion batteries based on combination Gaussian process functional regression.* Microelectronics Reliability, 2013. **53**(6): p. 832-839.

26. Li, L., et al., *Remaining Useful Life Prediction for Lithium-Ion Batteries Based on Gaussian Processes Mixture.* PloS one, 2016. **11**(9): p. e0163004-e0163004.

27. Cho, S., et al., *State-of-charge estimation for lithium-ion batteries under various operating conditions using an equivalent circuit model.* Computers & Chemical Engineering, 2012. **41**: p. 1-9.

28. Catti, M. and M. Montero-Campillo, *First-principles modelling of lithium iron oxides as battery cathode materials.* Journal of Power Sources, 2011. **196**(8): p. 3955-3961.

29. Verbrugge, M.W., P. Liu, and S. Soukiazian, *Activated-carbon electric-double-layer capacitors: electrochemical characterization and adaptive algorithm implementation.* Journal of Power Sources, 2005. **141**(2): p. 369-385.

30. Hu, X., S. Li, and H. Peng, *A comparative study of equivalent circuit models for Li-ion batteries.* Journal of Power Sources, 2012. **198**: p. 359-367.

31. M.W. Verbrugge, R.S.C., *Electrochemical and Thermal Characterization of battery Modules Commensurate with Electric Vehicle Intergration.* Electrochimica Acta, 2002. **149**: p. A45-A53.

32. Cacciato, M., et al., *Real-Time Model-Based Estimation of SOC and SOH for Energy Storage Systems.* IEEE Transactions on Power Electronics, 2017. **32**(1): p. 794-803.

33. Le, D. and X. Tang. *Lithium-ion battery state of health estimation using Ah-V characterization*. in *Proceedings of the Annual Conference of Prognostics and Health Management (PHM) Society, Montreal, QC, Canada*. 2011.

34. Lu, L., et al., *A review on the key issues for lithium-ion battery management in electric vehicles.* Journal of Power Sources, 2013. **226**: p. 272-288.

35. Baghdadi, I., et al., *State of health assessment for lithium batteries based on voltage–time relaxation measure.* Electrochimica Acta, 2016. **194**: p. 461-472.

36. Seinfeld, M.H.a.J.H., *Observability of Nonlinear system.* Optimization Theory and Application, 1987. **10(2)**: p. 67-77.

37. Plett, G.L., *Extended Kalman filtering for battery management systems of LiPB-based HEV battery packs: Part 2. Modeling and identification.* Journal of Power Sources, 2004. **134**(2): p. 262-276.

38. Kim, I.-S., *The novel state of charge estimation method for lithium battery using sliding mode observer.* Journal of Power Sources, 2006. **163**(1): p. 584-590.

39. Chen, X., et al., *Sliding Mode Observer for State of Charge Estimation Based on Battery Equivalent Circuit in Electric Vehicles.* Australian Journal of Electrical and Electronics Engineering, 2012. **9**(3): p. 225-234.

40. *Pipeline Corrosion Integrity Management*. 2009, NACE International.

41. Li, K.F.T.a.C.Q. *A numerical study of maintenance strategy for concrete structures in marine environment*. in *11th International Conference on Applications of Statistics and Probability in Civil Engineering*. 2011. Zurich, Switzerland.

42. Khan, K.F.T.a.L.R. *Risk-Cost Optimization and Reliability Analysis of Underground pipelines*. in *6th International ASRANet Conference*. 2012. London, UK.

43. H.O, M., *Method of structural Safety*. 1986, Prentice-Hall: Englewood Cliffs.

44. Kiefner J.F and Vieth, P.H., *A modified Criterion for Evaluating the Remaining Strength of Corroded Pipe.*, in *Project PR-3-805*. 1999, Pipeline Corrosion Supervisory Committee of the pipeline Research Committee of the American Gas Association.

45. Q.Chen, M.N., *Reliability based Prevention of Mechanical Damage to Pipelines*, in *PR-244-9729*. 1999, Pipeline Research Council International.

46. Tom Zimmerman, M.N., Martin McLamb. *Target Reliability Levels for Onshore Gas Pipelines*. in *4th International Pipeline Conference*. 2002. Calgary, Alberta, Canada.

47. Maher Nessim, W.Z., *Target Reliability Levels for the Design and Assessment of onshore Natural Gas Pipelines*. 2005, Gas Research Institute: C-FER Technologies.

48. Mark Stephens, M.N., *A Comprehensive approach to corrosion management based on structural reliability methods*, in *6th International Pipeline Conference*. 2006: Calgary, Alberta, Canada.

49. Q.Chen, M.N., *Reliability based Prevention of Mechanical Damage to Pipelines*. 1999, Pipeline Research Council International C-FER Technologies.

50. Stephens, M.J., *A Model for sizing high consequence areas associated with Natural Gas pipelines*. 2000, Gas Research Institute: C-FER Technologies.

51. Jr, M.B., *Potential Impact Radius Formulae for Flammable Gases other than Natural Gas Subject to 49 CFR 192*. 2005, C-FER Technologies.

52. Baker, M., *Derivation of Potential Impact Radius Formulae for vapor cloud dispersion subject to 49 CFR 192*. 2005, Department of Transportation.

53. Li, H.-S., Y.-Z. Ma, and Z. Cao, *A generalized Subset Simulation approach for estimating small failure probabilities of multiple stochastic responses.* Computers & Structures, 2015. **153**: p. 239-251.

54. Xie, M. and Z. Tian, *A review on pipeline integrity management utilizing in-line inspection data.* Engineering Failure Analysis, 2018. **92**: p. 222-239.

55. Vanaei, H.R., A. Eslami, and A. Egbewande, *A review on pipeline corrosion, in-line inspection (ILI), and corrosion growth rate models.* International Journal of Pressure Vessels and Piping, 2017. **149**: p. 43-54.

56. Zhou, Q., et al., *Estimation of corrosion failure likelihood of oil and gas pipeline based on fuzzy logic approach.* Engineering Failure Analysis, 2016. **70**: p. 48-55.

57. Jana, D.K., et al., *Novel type-2 fuzzy logic approach for inference of corrosion failure likelihood of oil and gas pipeline industry.* Engineering Failure Analysis, 2017. **80**: p. 299-311.

58. Guzman Urbina, A. and A. Aoyama, *Measuring the benefit of investing in pipeline safety using fuzzy risk assessment.* Journal of Loss Prevention in the Process Industries, 2017. **45**: p. 116-132.

59. Provan, J.W. and E.S.R. III, *Part I: Development of a Markov Description of Pitting Corrosion.* CORROSION, 1989. **45**(3): p. 178-192.

60. Association, C.S., *Oil and gas pipeline systems*, in *Commentary on CSA Z662-07*.

61. Tee, K.F., et al., *Reliability based life cycle cost optimization for underground pipeline networks.* Tunnelling and Underground Space Technology, 2014. **43**: p. 32-40.

62. Caleyo, F., et al., *Markov chain modelling of pitting corrosion in underground pipelines.* Corrosion Science, 2009. **51**(9): p. 2197-2207.

63. Laggoune, R., A. Chateauneuf, and D. Aissani, *Opportunistic policy for optimal preventive maintenance of a multi-component system in continuous operating units.* Computers & Chemical Engineering, 2009. **33**(9): p. 1499-1510.

64. HSE, *Reducing risks protecting people HSE's decision-making process*. 2001.

65. *Guidance on Treatment of the Economic value of a statistical life (VSL) in U.S. Department of Transportation Analyses, 2016*

*adjustment*. 2016, U.S Department of Transportation: Office of the secretary of transportation.

66. *HSE's health and safety improvement measure*. 2007; Available from: http://www.hse.gov.uk/risk/theory/alarpcheck.htm.

67. DfT, a.J.H.a.H.S., *The costs to Britain of workplace accidents and work-related ill health in 1995/96*. 1995, HSE.

68. M.A. Nessim, M.J.S., *Consequence Estimation for onshore pipelines* 2001, C-FER Technologies.

Nomenclature

| | |
|---|---|
| $\rho_a$ | Actual defect density |
| $\hat{\Gamma}_i$, | Adaptive switching gain |
| $c_2$ | Additive model factor |
| $c_{ma}$ | Annual component of the maintenance cost |
| ALARP | As low as reasonably practicable |
| $d_{avg}$ | Average defect depth |
| $g_{davg}$ | Average depth grwoth rate constant |
| BMS | Battery management system |
| $N_i$ | Calculated number of defect excavations or repairs for pipeline |
| CSA | Canadian standard association |
| $F_{cp}$ | Capital recovery factor, |
| CIPS | Close interval potential survey |
| $z_u$ | Compressibility factor of the gas |
| $p_f$ | Conditional probability of failure given an occurrence of the event |
| Q | Constant characterizing tool accuracy |
| CBA | Cost benefit Analysis |
| $C_i$ | Cost of a defect excavation and repair and inspection |
| $C_{main}$ | Cost related to pipeline inspection, excavation, repair |
| $S_{cr}$ | Critical resistance with unstable axial defect growth |
| $K_{Ic}$ | Critical stress intensity |
| $l_t$ | Cross-sectional length of the indentor |
| $w_t$ | Cross-sectional width of the indentor |
| $F_t(\tau)$. | Cumulative probability distribution |
| CPPT | Current Pulse pattern test |
| $\tau_{davg0}$ | Depth growth time delay constant |
| DCVG | Direct current voltage gradient |
| $C_d$ | Discharge coefficient |
| $R_d$ | Dynamic impact factor |
| D | Effective hole diameter |

| | |
|---|---|
| $Q_{eff}$ | Effective release rate |
| H | Efficiency factor |
| E | Elastic modulus |
| EV | Electric vehicle |
| $X_g$ | Emissivity factor |
| ESS | Energy storage system |
| ECM | Equivalent Circuit model |
| EGIG | European Gas Pipeline Incident Data Group |
| w | Excavator mass |
| EM | Expectation and Maximization |
| EKF | Extended kalman filtering |
| ECDA | External Corrosion Direct Assessment |
| $\lambda_f$ | Failure probability |
| FORM | First order Reliability Method |
| $\Phi$ | Flow factor |
| M | Folias factor. |
| $\Omega$ | Frequency of failure occurrence event |
| F | Friction factor |
| $C_v$ | Full size Charpy V notch palteau energy |
| GRI | Gas Research Institute |
| $d_g$ | Gouge depth |
| GC | Graphite copolymer |
| HSE | Health and Safety Executive |
| I | Heat Flux |
| $H_c$ | Heat of combustion |
| $\sigma_c$ | Hoop stress |
| HEV | Hybrid Electric Vehicle |
| $p_i$ | Ignition probability |
| IMP | Integrity Management Program |
| KEPCO | Korea electric power corporation |
| KEEI | Korea Energy Economics Institute |
| KTC | Korea Testing Certificate |

| | |
|---|---|
| $g_{l0}$ | Length growth rate at the time prior maintenance action |
| $g_l$ | Length growth rate at time of interested time |
| $\tau_{l0}$ | length growth time delay constant |
| $A_c$ | Ligament of full size Charpy specimens |
| LTI | Linear time invariant |
| LCO | Lithium Cobalt Oxide (LiCoO2) |
| LFP | Lithium iron phosphate (LiFePO 4) |
| LMO | Lithium Mangaese Oxide |
| NCA | Lithium Nickel Cobalt Aluminium Oxide (LiNiCoAlO2) |
| LiNMC | Lithium-nickel-manganese-cobalt oxide(LiNiCoMnO2) |
| MCMCS | Markov chain monte carlo simulation |
| $l(\tau)$ | Maximum axial defect length at time |
| $d_{max}$ | Maximum defect depth |
| $p_{max}$ | Maximum permissible failure rate |
| MSE | Mean square error |
| $\rho_d$ | Measure density of detected defects |
| E | Model error term |
| MCS | Monte carlo simulation |
| $c_1$ | Multiplicative model error factor |
| NCM | Nickel cobalt manganese(LiNiCoMnO2) |
| c | One-half the defect length |
| OCV | Open circuit voltage |
| $Q_{in}$ | Peak release rate |
| $r_a$ | Pipe resistance |
| PHMSA | Pipeline and Hazardous Materials Safety Administration. |
| $p_d$ | Probability of detecting a randomly selected defect |
| $p_{fi}$ | Probability that a given defect indication is false |
| $P_{in}$ | Proportions of time spent indoor |
| $P_{out}$ | Proportions of time spent outdoor |
| RLS | Recursive least square |
| $t_r$ | Reduced time |
| $\lambda$ | Release rate decay factor |

| | |
|---|---|
| $R_T$ | Reliability target |
| SORM | Second order Reliability Method |
| SMO | Sliding mode observer |
| $a_0$ | Sonic velocity of gas |
| SOC | State of charge |
| SOH | State of Health |
| SRA | Structural Reliability Assessment |
| $\Gamma$ | Subsequent defect accumulation rate. |
| SS | Subset simulation |
| SSE | Sum of square error |
| $\sigma_u$ | Tensile strength |
| $R_N$ | The normal load factor |
| T | Time elapsed since interested time |
| $n_l$ | Time exponent for length growth rate |
| $n_{davg}$ | Time exponent for the depth growth rate |
| $t_{release}$ | Time from pipe damage |
| $r_{max}$ | Tolerable level of risk |
| t | Wall thickness |
| S | Yield strength |